

*Supporting Information for*

**Three-Dimensional Covalent Organic Frameworks Based on  
 $\pi$ -Conjugated Tetrahedral Node**

Miaomiao Wu,<sup>a</sup> Zhen Shan,<sup>a</sup> Jinjian Wang,<sup>a</sup> Zhangjie Gu,<sup>a</sup> Xiaowei Wu,<sup>a</sup> Bingqing Xu,<sup>a</sup> Gen Zhang<sup>\*a</sup>

<sup>a</sup> Key Laboratory for Soft Chemistry and Functional Materials of Ministry of Education, School of Chemical Engineering, Nanjing University of Science and Technology, Nanjing, Jiangsu 210094, China.

This work dedicated to Professor Susumu Kitagawa on the occasion of his 70th birthday.

E-mail: [zhanggen@njust.edu.cn](mailto:zhanggen@njust.edu.cn)

## Table of Content

1. Materials and methods.....	4
2. Synthesis and general procedures.....	5
2.1. Synthesis of COTh-CHO.....	5
Fig. S1 $^1\text{H}$ NMR spectra of COTh.....	7
Fig. S2 $^1\text{H}$ NMR spectra of COTh-4Br .....	7
Fig. S3 $^1\text{H}$ NMR spectra of COTh-CHO.....	8
Fig. S4 HRMS spectra of COTh-CHO.....	8
2.2. Synthesis of NUST-COFs.....	9
3. Characterization.....	11
Fig. S5 FT-IR spectra of COF-NUST-11, DAB-Me, and COTh-CHO.....	11
Fig. S6 FT-IR spectra of COF-NUST-12, DBDA-Me, and COTh-CHO.....	11
Fig. S7 FT-IR spectra of COF-NUST-13, TAPPy, and COTh-CHO .....	12
Fig. S8 $^{13}\text{C}$ Solid-State NMR spectrum of COF-NUST-11 .....	12
Fig. S9 $^{13}\text{C}$ Solid-State NMR spectrum of COF-NUST-12 .....	13
Fig. S10 $^{13}\text{C}$ Solid-State NMR spectrum of COF-NUST-13 .....	13
Fig. S11 TGA curves of COF-NUST-X (X = 11, 12, 13) .....	14
Table S1. Element analysis value of COF-NUST-11.....	14
Table S2. Element analysis value of COF-NUST-13.....	14
Fig. S12 SEM images of COF-NUST-11 .....	15
Fig. S13 SEM images of COF-NUST-12 .....	15
Fig. S14 SEM images of COF-NUST-13 .....	15
Fig. S15 TEM images of COF-NUST-11 .....	15
Fig. S16 TEM images of COF-NUST-12 .....	16
Fig. S17 TEM images of COF-NUST-13 .....	16
Fig. S18 PXRD patterns of COF-NUST-11, DAB-Me, and COTh-CHO .....	16
Fig. S19 PXRD patterns of COF-NUST-12, DBDA-Me, and COTh-CHO .....	17
Fig. S20 PXRD patterns of COF-NUST-13, TAPPy, and COTh-CHO .....	17
Fig. S21 PXRD patterns of COF-NUST-12. PXRD profiles of experimental pattern (red curves), Pawley refined (black curves), calculated (green curves) patterns, and their difference (gray curves) .....	18
Fig. S22 Calculated PXRD pattern of COF-NUST-11 based on the 8-, 9- and 10- fold interpenetration of <i>dianet</i> .....	18
Fig. S23 Calculated PXRD pattern of COF-NUST-12 based on the 12-, 13- and 14- fold interpenetration of <i>dianet</i> .....	19
Fig. S24 Calculated PXRD pattern of COF-NUST-13 based on the non- and 2- fold interpenetration of <i>pts</i> net .....	19
Fig. S25 PXRD patterns of COF-NUST-11 after soaked in different solvents for 72 h .....	20
Fig. S26 PXRD patterns of COF-NUST-13 at different temperatures .....	20
Fig. S27 $\text{N}_2$ adsorption-desorption isotherms at 77 K of COFs .....	21
Fig. S28 Pore size distribution of COF-NUST-11 .....	21
Fig. S29 Pore size distribution of COF-NUST-12 .....	22
Fig. S30 Pore size distribution of COF-NUST-13 .....	22
Fig. S31 UV/vis spectra of COFs powders.....	23
Fig. S32 Fluorescence emission spectra of COTh-CHO, COF-NUST-11/12/13 powders ( $\lambda_{\text{ex}} = 360$ nm).....	23

Fig. S33 Fluorescence emission spectra of acetonitrile suspension of COF-NUST-11 upon increasing addition of (a) DNB and (b) NP ( $\lambda_{ex} = 360$ nm).....	24
Fig. S34 Fluorescence emission spectra of acetonitrile suspension of COF-NUST-11 upon increasing addition of (a) DNP and (b) NB ( $\lambda_{ex} = 360$ nm).....	24
Fig. S35 Fluorescence emission spectra of acetonitrile suspension of COF-NUST-11 upon increasing addition of (a) NT and (b) DNT ( $\lambda_{ex} = 360$ nm).....	24
Fig. S36 Fluorescence emission spectra of acetonitrile suspension of COF-NUST-11 upon increasing addition of TNP ( $\lambda_{ex} = 360$ nm).....	25
Fig. S37 Fluorescence emission spectra of acetonitrile suspension of COF-NUST-12 upon increasing addition of (a) DNB and (b) NP ( $\lambda_{ex} = 360$ nm).....	25
Fig. S38 Fluorescence emission spectra of acetonitrile suspension of COF-NUST-12 upon increasing addition of (a) DNP and (b) NB ( $\lambda_{ex} = 360$ nm).....	25
Fig. S39 Fluorescence emission spectra of acetonitrile suspension of COF-NUST-12 upon increasing addition of (a) NT and (b) DNT ( $\lambda_{ex} = 360$ nm).....	26
Fig. S40 Fluorescence emission spectra of acetonitrile suspension of COF-NUST-12 upon increasing addition of TNP ( $\lambda_{ex} = 360$ nm).....	26
Fig. S41 Fluorescence emission spectra of acetonitrile suspension of COF-NUST-13 upon increasing addition of (a) DNB and (b) NP ( $\lambda_{ex} = 360$ nm).....	26
Fig. S42 Fluorescence emission spectra of acetonitrile suspension of COF-NUST-13 upon increasing addition of (a) DNP and (b) NB ( $\lambda_{ex} = 360$ nm).....	27
Fig. S43 Fluorescence emission spectra of acetonitrile suspension of COF-NUST-13 upon increasing addition of (a) NT and (b) DNT ( $\lambda_{ex} = 360$ nm).....	27
Fig. S44 The Stern-Volmer plots obtained from titration of COF-NUST-11 with picric acid.....	27
Fig. S45 The Stern-Volmer plots obtained from titration of COF-NUST-12 with picric acid.....	28
Fig. S46 The Stern-Volmer plots obtained from titration of COF-NUST-13 with picric acid.....	28
Fig. S47 Fluorescence quenching (%) of acetonitrile suspension of COF-NUST-11 with various nitroaromatics at a concentration of 100 $\mu$ M.....	28
Fig. S48 Fluorescence quenching (%) of acetonitrile suspension of COF-NUST-12 with various nitroaromatics at a concentration of 100 $\mu$ M.....	29
Table S3. Fractional atomic coordinates for simulated COF-NUST-11 powders.....	29
Table S4. Fractional atomic coordinates for simulated COF-NUST-12 powders.....	31
Table S5. Fractional atomic coordinates for simulated COF-NUST-13 powders.....	33
Reference.....	36

## 1. Materials and methods

All the chemicals are commercially available, and used without further purification. All solvents were dried and distilled according to conventional methods. Compounds **1**, **2**, **3** and **COTh-4TMS** were synthesized according to the reported literature.<sup>[S1-3](#)</sup>

**Powder X-ray diffraction (PXRD):** PXRD patterns were collected on a Bruker D8 Advance diffractometer using Cu K $\alpha$  radiation.

**Fourier transform infrared (FT-IR):** FT-IR spectrum was measured on a Thermo Fisher Scientific Optics NICOLETIS10 FT-IR spectrometer with Universal ATR accessory between the ranges of 4000 to 525 cm $^{-1}$ .

**Solution nuclear magnetic resonance (NMR):** Liquid state  $^1\text{H}$  nuclear magnetic resonance spectroscopy was collected on a Bruker Avance III instrument with AS500 magnet equipped with a cryoprobe (500 MHz).

**High resolution mass spectrometry (HRMS):** HRMS mass spectra were collected on a Baird Acuity UPLC/XEVO G2-XS QTOF using CHCl $_3$  as a solvent.

**Elemental analysis:** The elemental analysis was conducted with the elemental analysizer FLASHSMART.

**Scanning electron microscope (SEM):** SEM images were collected using a JSM-IT500HR system.

**Transmission electron microscope (TEM):** TEM images were obtained with a JEM-2100, JEOL.

**Gas adsorption:** Gas adsorption measurement N $_2$  adsorption and desorption measurements were performed at 77 K using ASAP 2020, Micromeritics Instrument Corp, USA. Pore size distributions and pore volumes were derived from the adsorption isotherms.

**Thermogravimetric analysis (TGA):** TGA was performed using a TGA/SDTA851E, Mettler Toledo, under flowing N $_2$  (60 mL min $^{-1}$ ) with 10 K min $^{-1}$  ramp rate. Samples were heated in a Platinum pan from 50 °C to 900 °C.

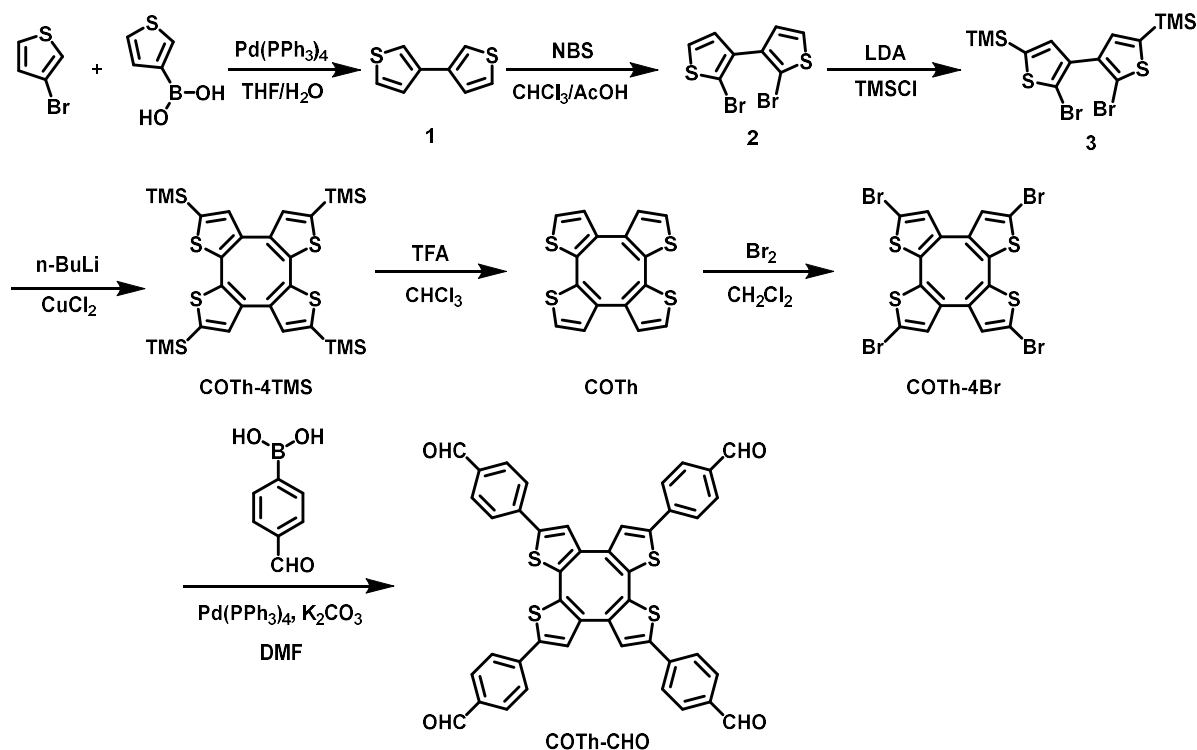
**UV-Vis spectroscopy (UV-vis):** The UV-vis spectra of COFs powders were collected using LAMBDA950, PerkinElmer, Germany.

**Fluorescence measurement:** The fluorescence spectra of samples were collected using

RF-5301PC. As for fluorescence detection of COFs with picric acid, 2 mg COFs powders were dispersed in 40 mL acetonitrile by ball-milling overnight, and after standing for 3 days, the homogeneous acetonitrile suspensions of the COFs were obtained. The fluorescence measurement of 2 mL acetonitrile suspensions was immediately carried out after gradual adding of 0  $\mu$ M, 10  $\mu$ M, 20  $\mu$ M, 30  $\mu$ M, 40  $\mu$ M, 50  $\mu$ M, 60  $\mu$ M, 70  $\mu$ M, 80  $\mu$ M, 90  $\mu$ M, and 100  $\mu$ M various nitroaromatics, respectively. The excitation wavelength used in the experiments was 360 nm, the width of excitation and launching slit were both 5.0 nm, and the scan speed was 500 nm/min.

## 2. Synthesis and general procedures

### 2.1. Synthesis of 4,4',4'',4'''-(cycloocta[1,2-b:4,3-b':5,6-b'':8,7-b'']tetrathiophene-2,5,8,11-tetrayl)tetrabenzaldehyde (COTh-CHO)



#### Synthesis of cycloocta[1,2-b:4,3-b':5,6-b'':8,7-b'']tetrathiophene (COTh).

COTh was synthesized according to the reported literature with a modified procedure.<sup>S1,3</sup> To a 50 mL round-bottom flask, COTh-4TMS (617 mg, 1 mmol) was dissolved in 20 mL  $\text{CHCl}_3$ , and trifluoroacetic acid (TFA, 1 mL) was added dropwise. The mixture reaction was stirred at room temperature for 1 h. Water was added to quench the reaction, the mixture was extracted with DCM

( $3 \times 50$  mL) and washed with aqueous  $\text{NaHCO}_3$  and  $\text{H}_2\text{O}$ . Then the solvent was removed under reduced pressure to afford COTh as yellow powders (315 mg, 96%).  **$^1\text{H NMR}$**  (500 MHz,  $\text{CDCl}_3$ ):  $\delta$  7.37 (d, 4H), 6.97 (d, 4H).

### Synthesis of 2,5,8,11-tetrabromocycloocta[1,2-b:4,3-b':5,6-b'':8,7-b'']tetrathiophene (COTh-4Br).

COTh-4Br was synthesized according to the reported literature with a modified procedure.<sup>1,3</sup> To a 100 mL round-bottom flask, COTh (600 mg, 1.8 mmol) was dissolved in 50 mL  $\text{CH}_2\text{Cl}_2$ , after cooling to 0 °C, bromine (1 mL) was added dropwise. Then the reaction mixture was slowly warmed up and kept stirring at room temperature for 48 h. Saturated aqueous  $\text{NaHSO}_3$  (10 mL) was added dropwise to quench the reaction, the mixture was extracted with DCM ( $3 \times 20$  mL) and washed with aqueous  $\text{NaHSO}_3$  and  $\text{H}_2\text{O}$ . Then the solvent was removed under reduced pressure to afford COTh-4Br as off-white powders (1.04 g, 88%).

### Synthesis of COTh-CHO.

To a 250 mL Schlenk tube, COTh-4Br (644 mg, 1 mmol), (4-formylphenyl)boronic acid (900 mg, 6 mmol), Tetratriphenylphosphor palladium (140 mg, 0.12 mmol), and potassium carbonate (2.55 g, 12 mmol) were added, then the flak was vacuumed for 30 minutes, during which argon gas was pumped three times. Under  $\text{N}_2$  atmosphere, 100 mL *N,N*-Dimethylformamide (DMF) was added to the tube. The reaction mixture was heated to 100 °C, and kept stirring at 100 °C for 48 h. After cooling to room temperature, the mixture was poured into 500 mL water and filtered. The crude product was recrystallization from  $\text{CH}_2\text{Cl}_2/\text{MeOH}$  to afford COTh-CHO as croci powders (275 mg, 37%).  **$^1\text{H NMR}$**  (500 MHz, DMSO):  $\delta$  10.02 (s, 4H), 7.99 (d, 8H), 7.98 (d, 8H), 7.95 (s, 4H). **ESI-HRMS:** calcd. for  $[\text{C}_{44}\text{H}_{24}\text{O}_4\text{S}_4 + \text{H}]$  744.05574, found 744.05743.

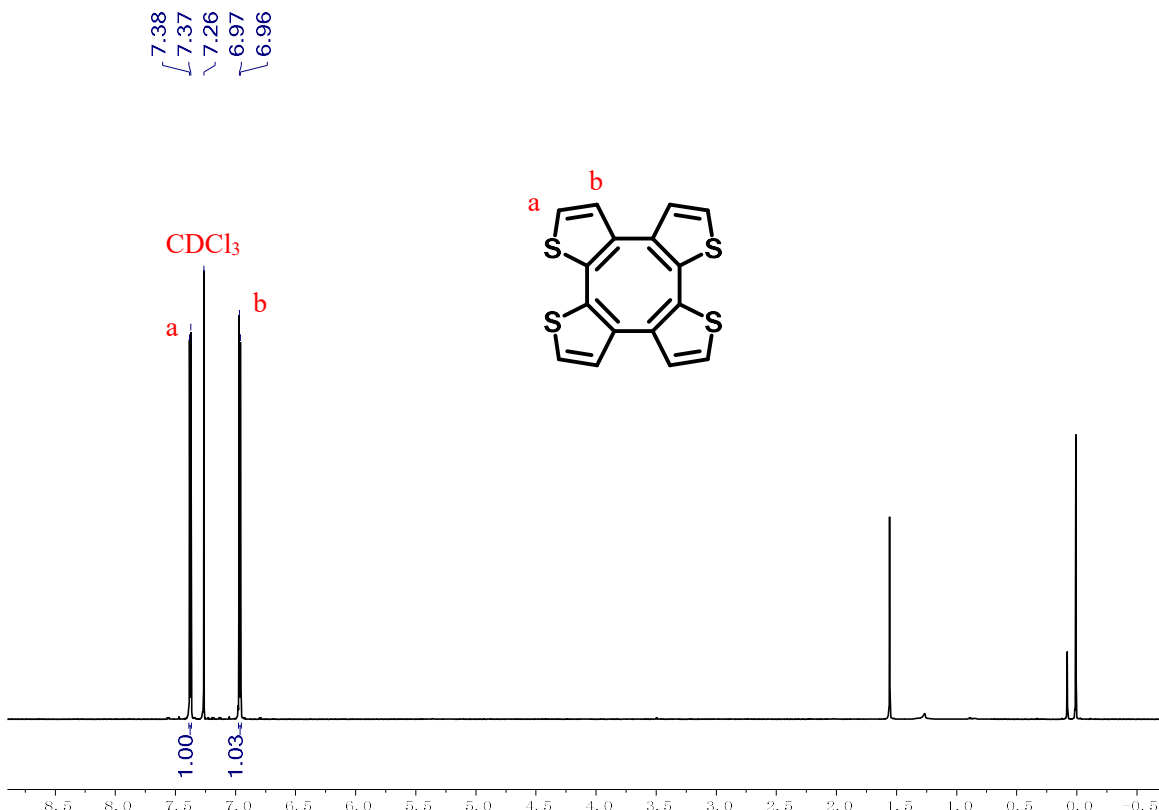


**Fig. S1**  $^1\text{H}$  NMR spectra of COTH

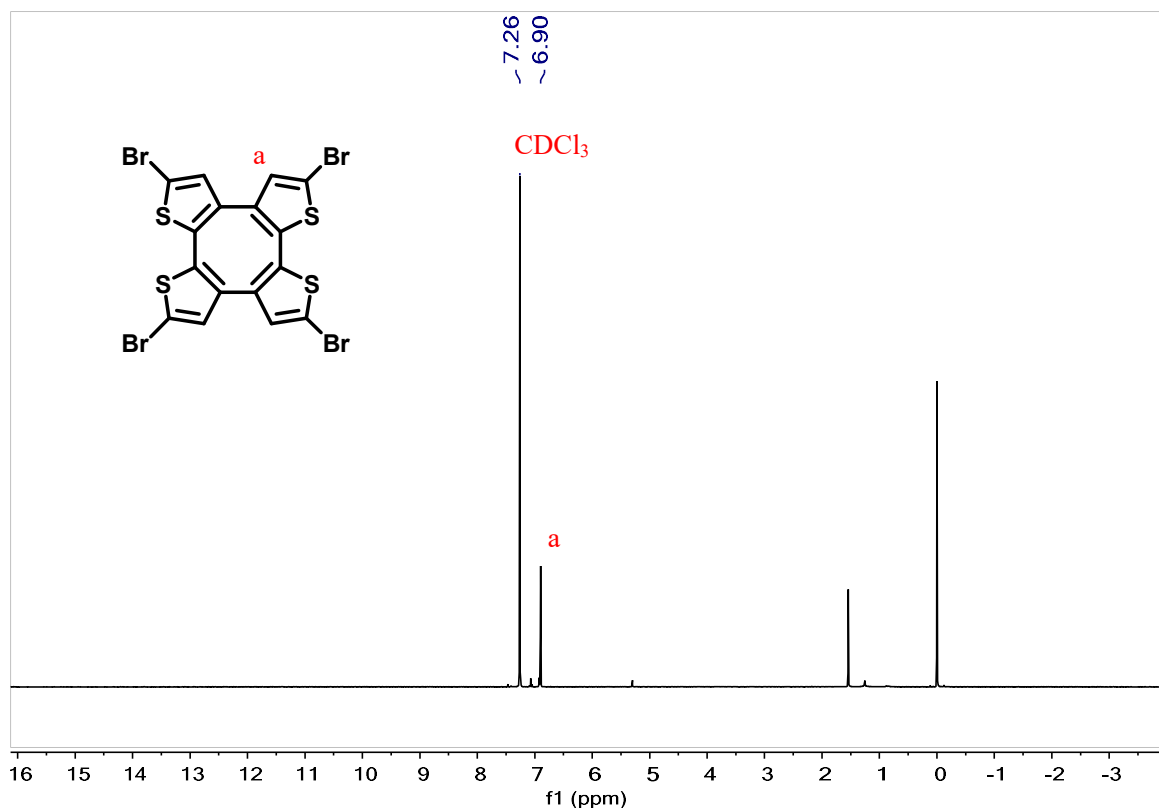


**Fig. S2**  $^1\text{H}$  NMR spectra of COTH-4Br

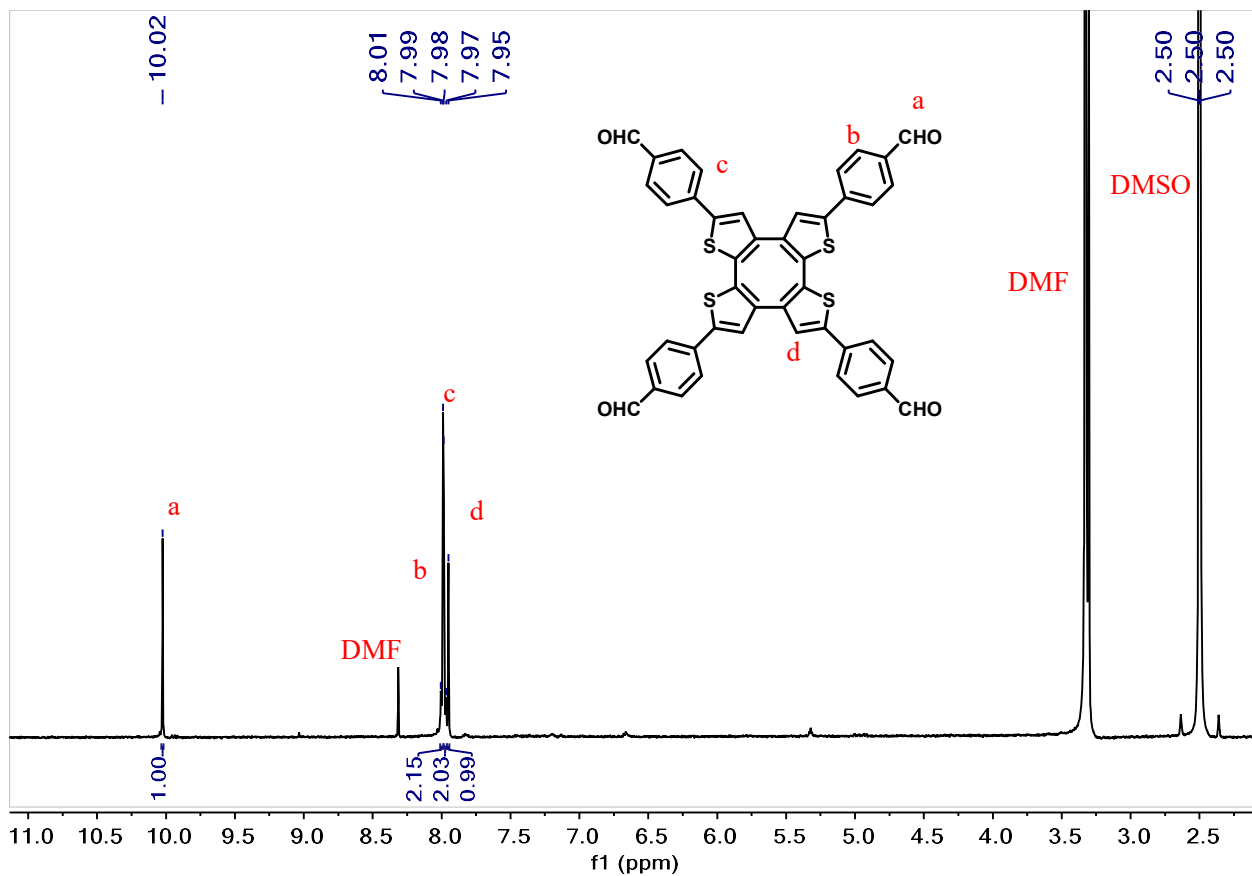


Fig. S3 <sup>1</sup>H NMR spectra of COTh-CHO

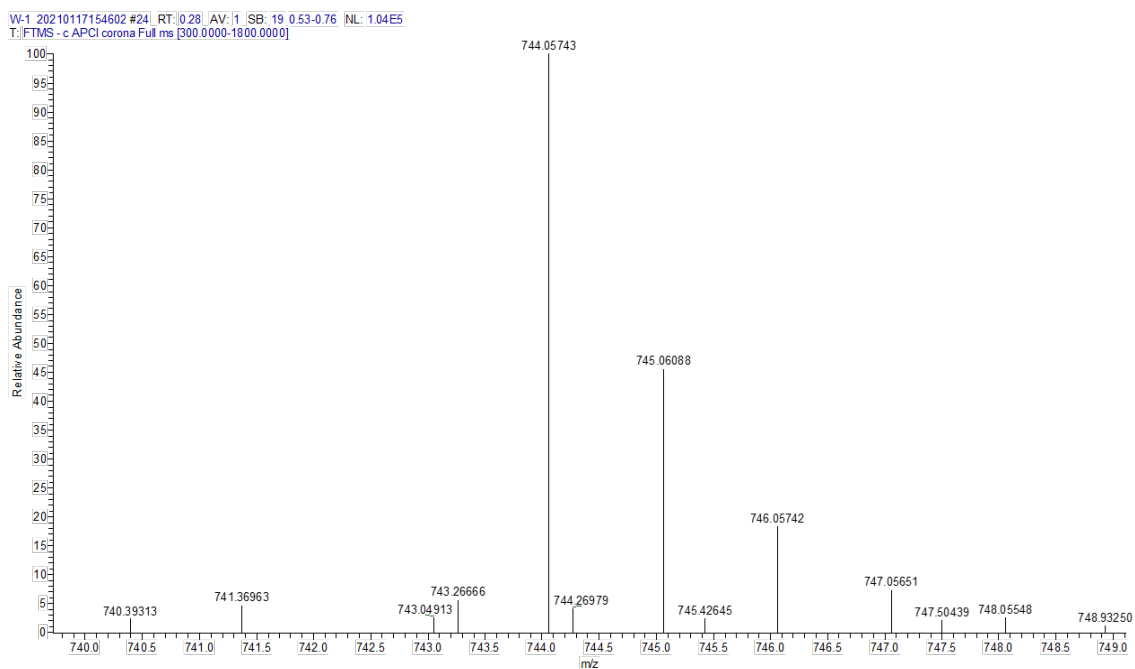
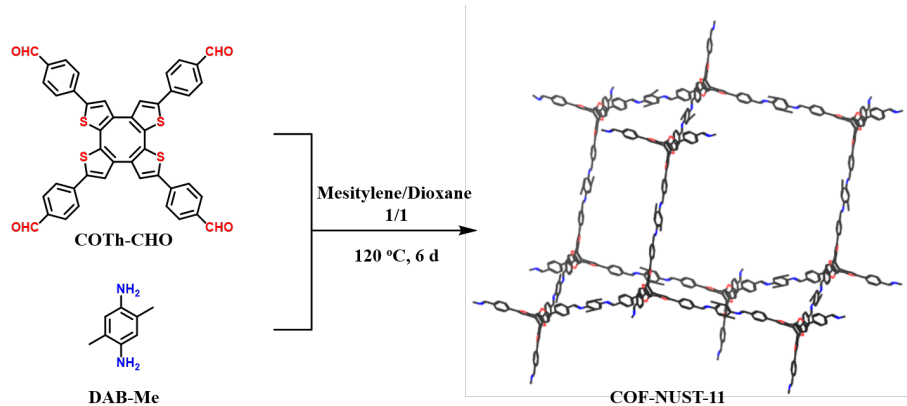


Fig. S4 HRMS spectra of COTh-CHO

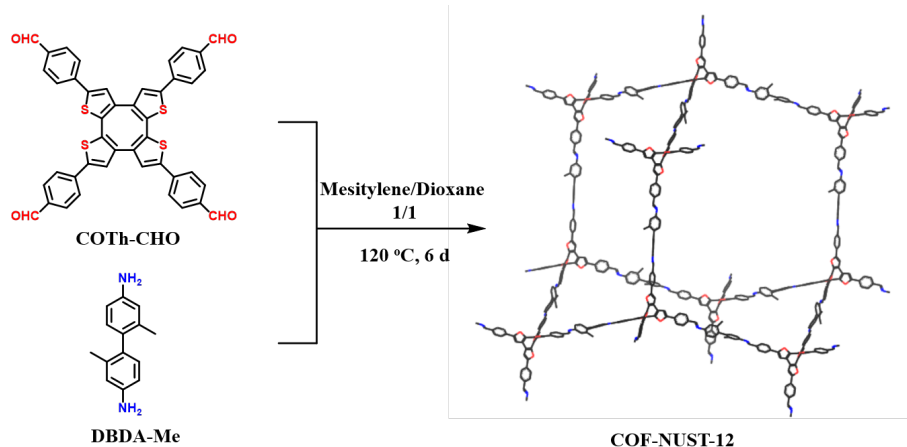
## 2.2. Synthesis of NUST-COFs

### Synthesis of COF-NUST-11



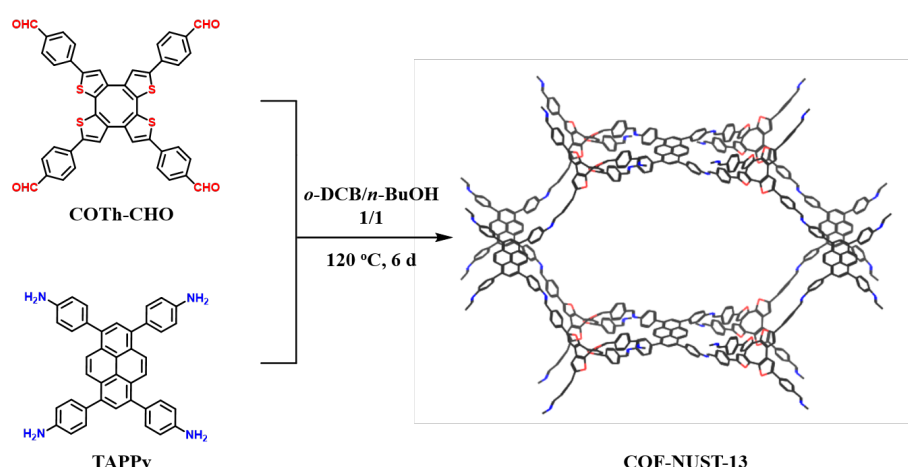
COTh-CHO (29.8 mg, 0.04 mmol) and 1,4-diamine-2,5-dimethylbenzene DAB-Me (10.9 mg, 0.08 mmol) were weighed into a Pyrex tube, then mesitylene (1.0 mL), dioxane (1.0 mL) were added. After ultrasound for 5 min, 6 M acetic acid (0.2 mL) was poured into the glass ampoule as catalyst. The ampoule was flash frozen in a liquid nitrogen bath and degassed through freeze-pump-thaw cycles for three times and flame sealed. Upon warming to room temperature, the ampoule was kept at 120 °C for 6 days in an oven to give orangered powders. The solid was isolated by filtration and washed with DMF (3×10 mL), acetone (3×10 mL), then the powders were soaking in 30 mL acetone for 12 h and filtered. The sample was dried at 80 °C under vacuum for 24 h to yield COF-NUST-11 (32 mg, 85%).

### Synthesis of COF-NUST-12



COTh-CHO (29.8 mg, 0.04 mmol) and 2,2'-dimethyl-[1,1'-biphenyl]-4,4'-diamine DBDA-Me (17.0 mg, 0.08 mmol) were weighed into a Pyrex tube, then mesitylene (1.0 mL), dioxane (1.0 mL) were added. After ultrasound for 5 min, 6 M acetic acid (0.2 mL) was poured into the glass ampoule as catalyst. The ampoule was flash frozen in a liquid nitrogen bath and degassed through freeze-pump-thaw cycles for three times and flame sealed. Upon warming to room temperature, the ampoule was kept at 120 °C for 6 days in an oven to give orangered powders. The solid was isolated by filtration and washed with DMF (3×10 mL), acetone (3×10 mL), then the powders were soaking in 30 mL acetone for 12 h and filtered. The sample was dried at 80 °C under vacuum for 24 h to yield COF-NUST-12 (36 mg, 82%).

### Synthesis of COF-NUST-13



COTh-CHO (22.4 mg, 0.03 mmol) and 1,3,6,8-tetrakis(4-aminophenyl)pyrene TAPPy (17.0 mg, 0.03 mmol) were weighed into a Pyrex tube, then *o*-dichlorobenzene (1.0 mL), *n*-butyl alcohol (1.0 mL) were added. After ultrasound for 5 min, 6 M acetic acid (0.2 mL) was poured into the glass ampoule as catalyst. The ampoule was flash frozen in a liquid nitrogen bath and degassed through freeze-pump-thaw cycles for three times and flame sealed. Upon warming to room temperature, the ampoule was kept at 120 °C for 6 days in an oven to give orangered powders. The solid was isolated by filtration and washed with DMF (3×10 mL), acetone (3×10 mL), then the powders were soaking in 30 mL acetone for 12 h and filtered. The sample was dried at 80 °C under vacuum for 24 h to yield COF-NUST-13 (29 mg, 78%).

### 3. Characterization

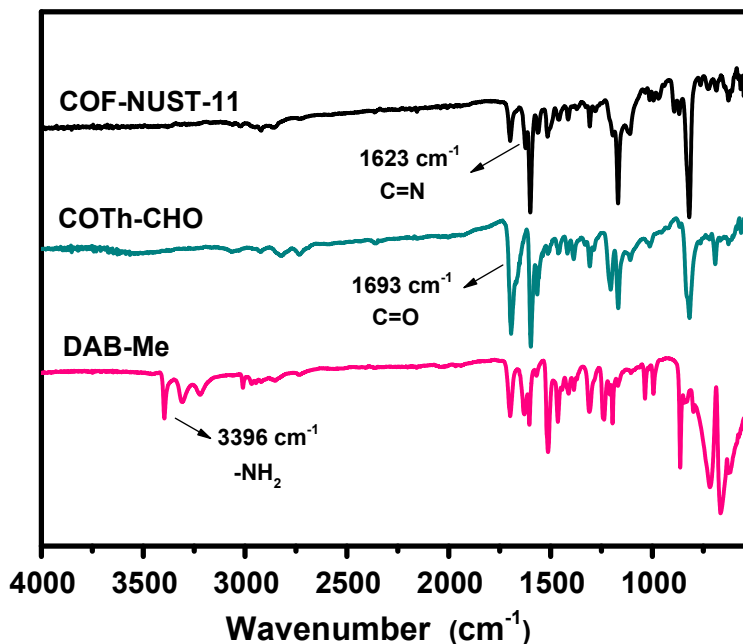


**Fig. S5** FT-IR spectra of COF-NUST-11, DAB-Me, and COTh-CHO

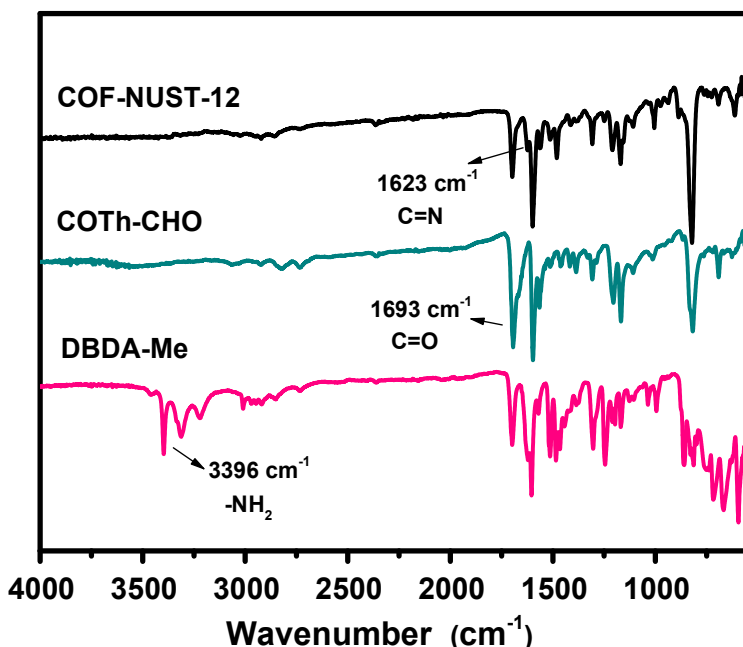


**Fig. S6** FT-IR spectra of COF-NUST-12, DBDA-Me, and COTh-CHO

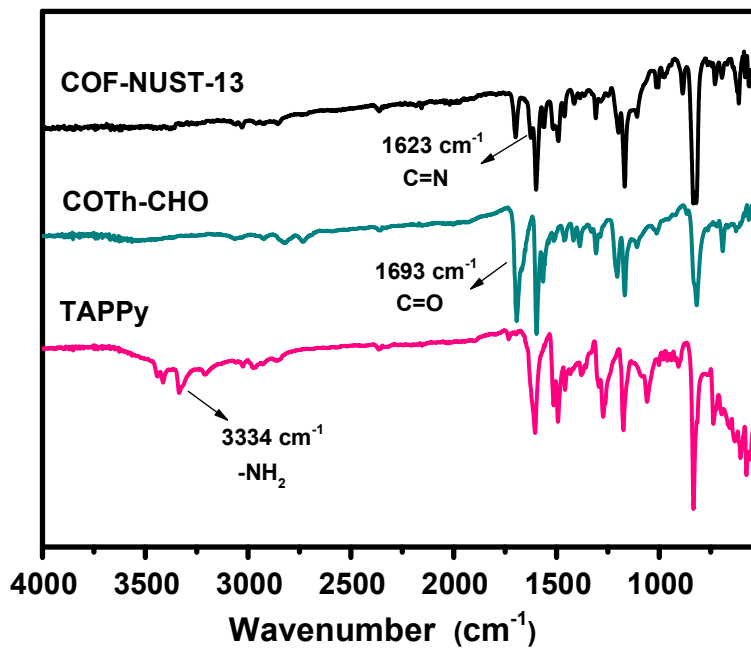


**Fig. S7** FT-IR spectra of COF-NUST-13, TAPPY, and COTh-CHO

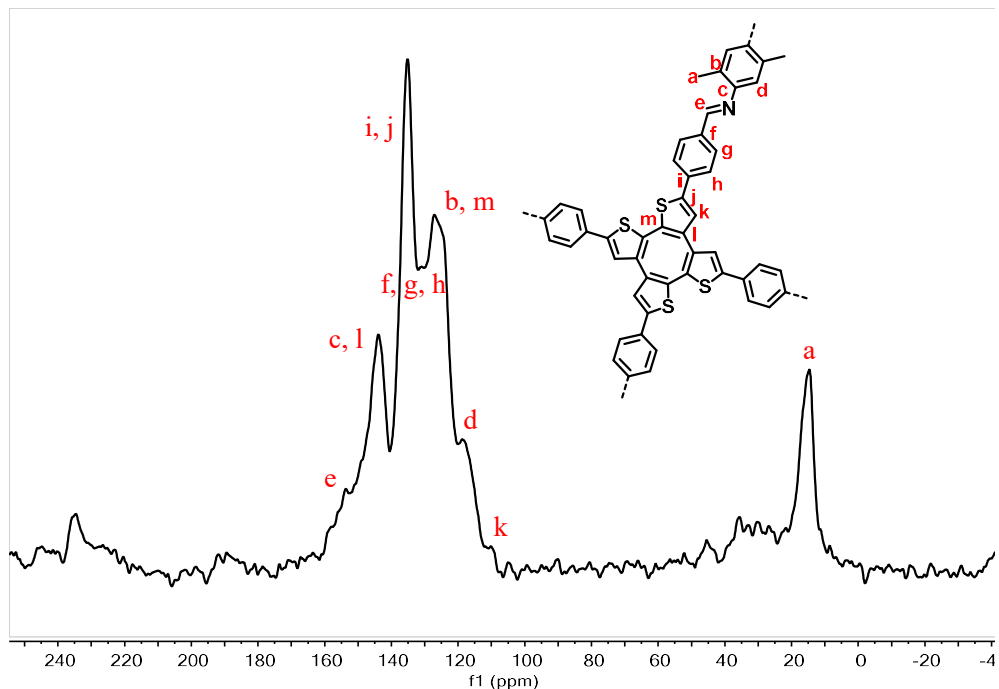


**Fig. S8**  $^{13}\text{C}$  Solid-State NMR spectrum of COF-NUST-11

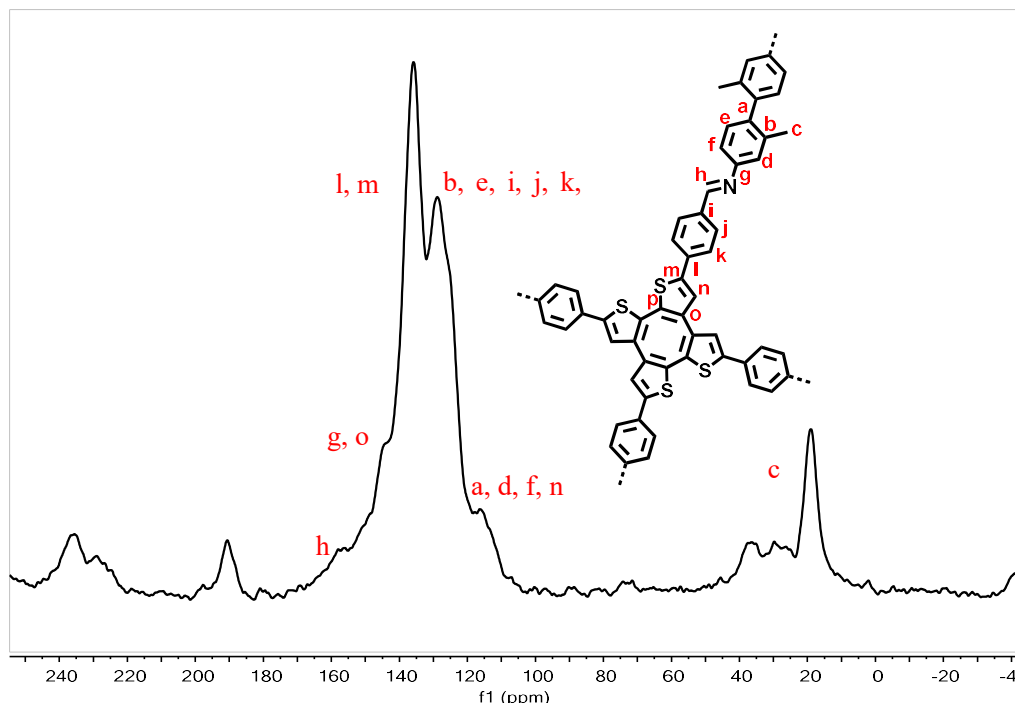


**Fig. S9**  $^{13}\text{C}$  Solid-State NMR spectrum of COF-NUST-12

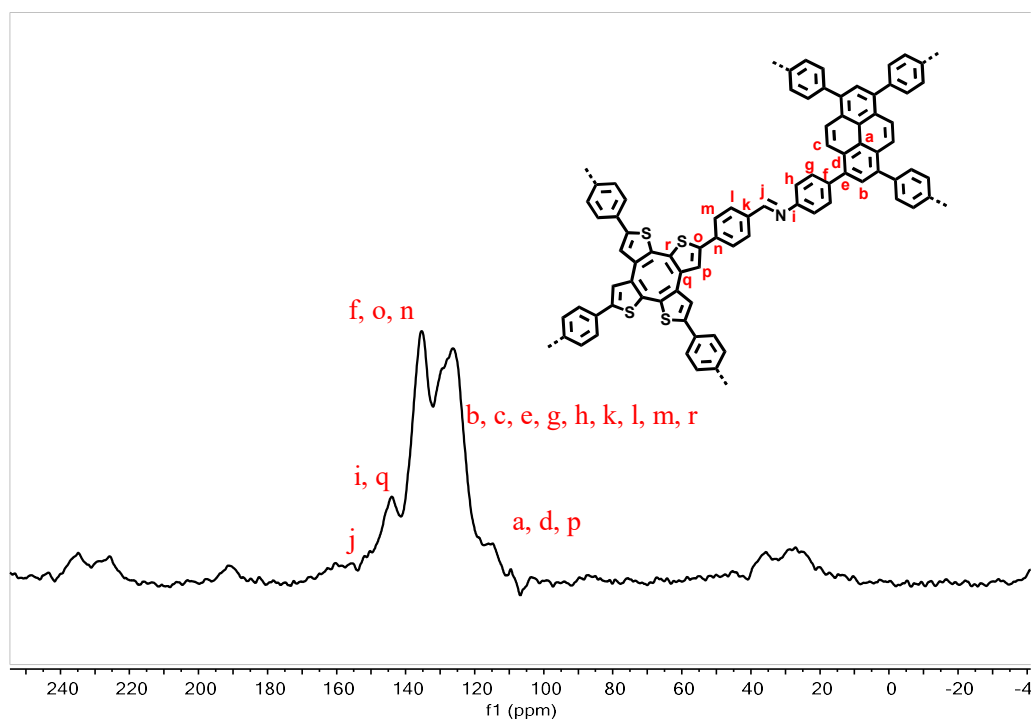


**Fig. S10**  $^{13}\text{C}$  Solid-State NMR spectrum of COF-NUST-13

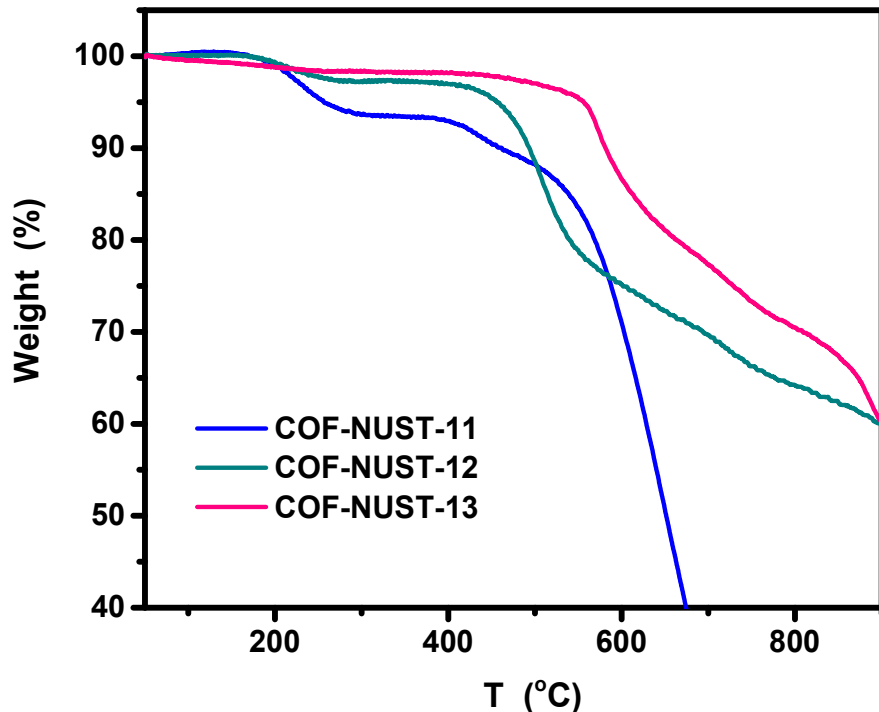


**Fig. S11** TGA curves of COF-NUST-X (X = 11, 12, 13)

**Table S1.** Element analysis value of COF-NUST-11

		C (%)	N (%)	H (%)	S (%)
COF-NUST-11	Theoretical	76.27	5.93	4.23	13.56
	Experimental	69.04	3.92	4.58	8.65

**Table S2.** Element analysis value of COF-NUST-13

		C (%)	N (%)	H (%)	S (%)
COF-NUST-13	Theoretical	81.42	4.52	3.71	10.34
	Experimental	73.43	3.34	3.63	9.32

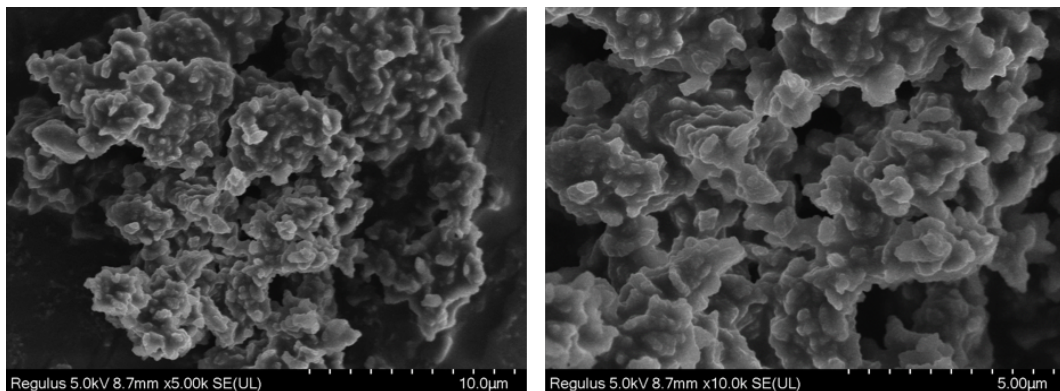


**Fig. S12** SEM images of COF-NUST-11

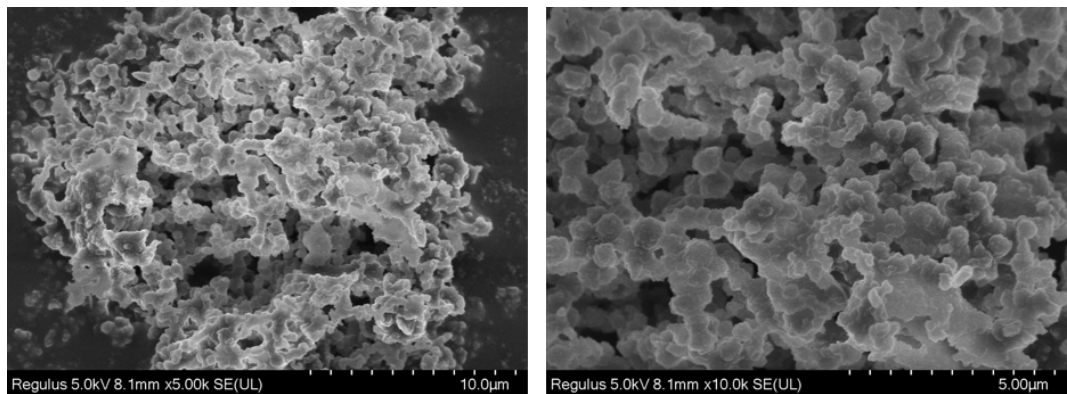


**Fig. S13** SEM images of COF-NUST-12

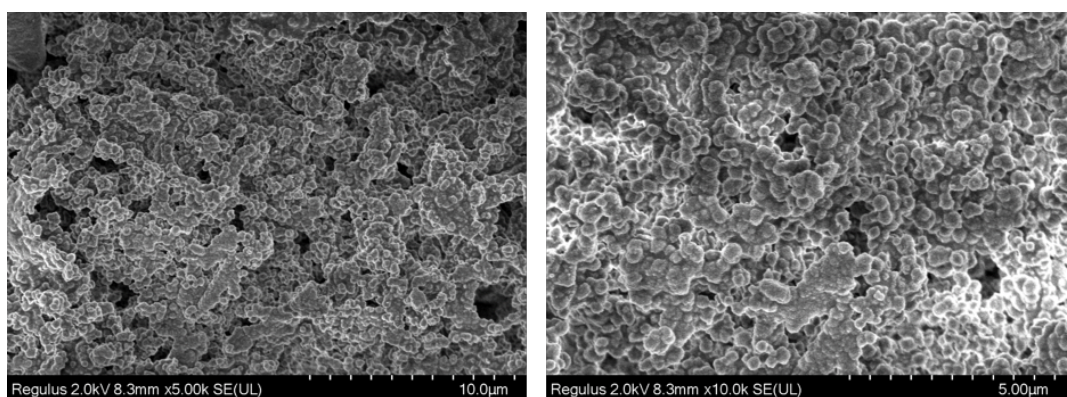


**Fig. S14** SEM images of COF-NUST-13

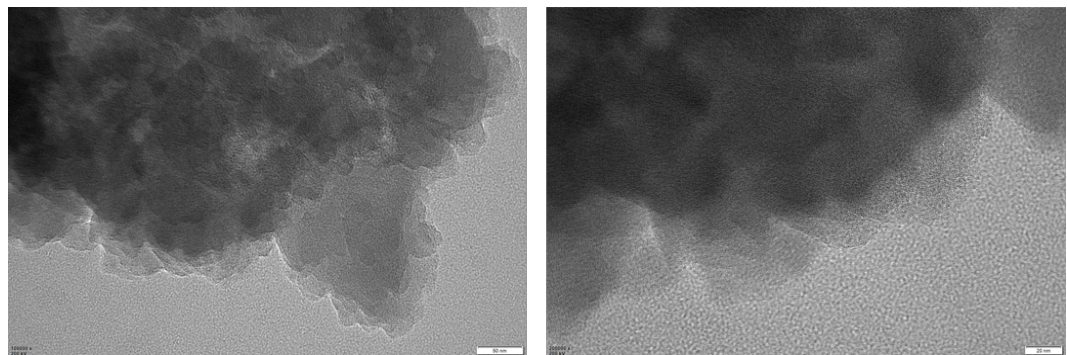


**Fig. S15** TEM images of COF-NUST-11

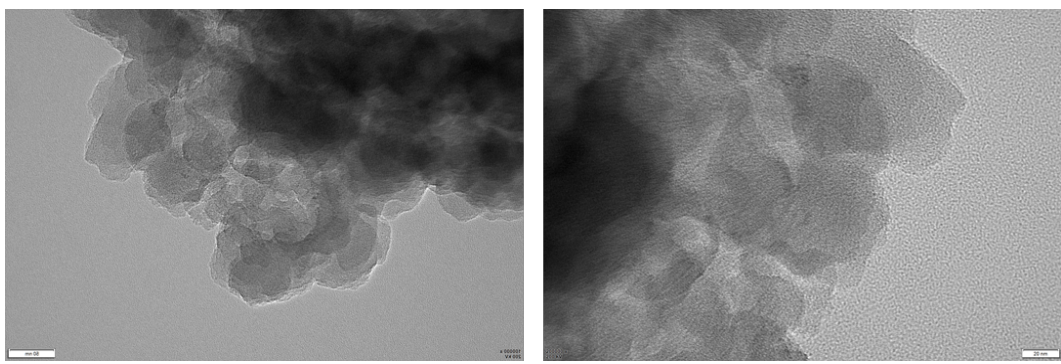


**Fig. S16** TEM images of COF-NUST-12

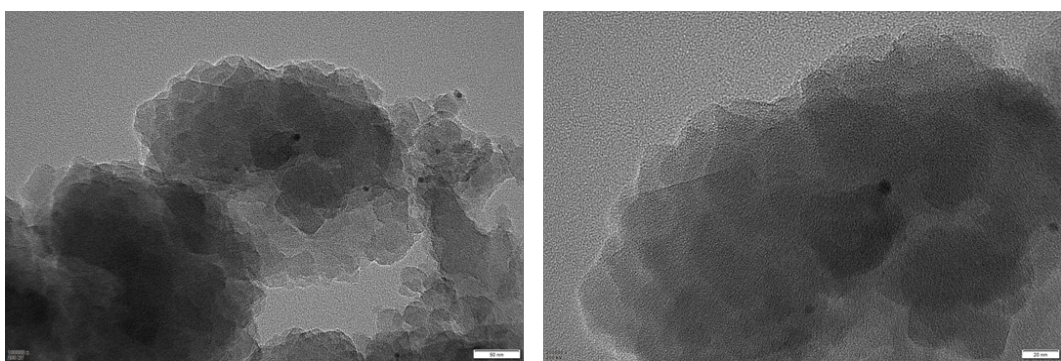


**Fig. S17** TEM images of COF-NUST-13

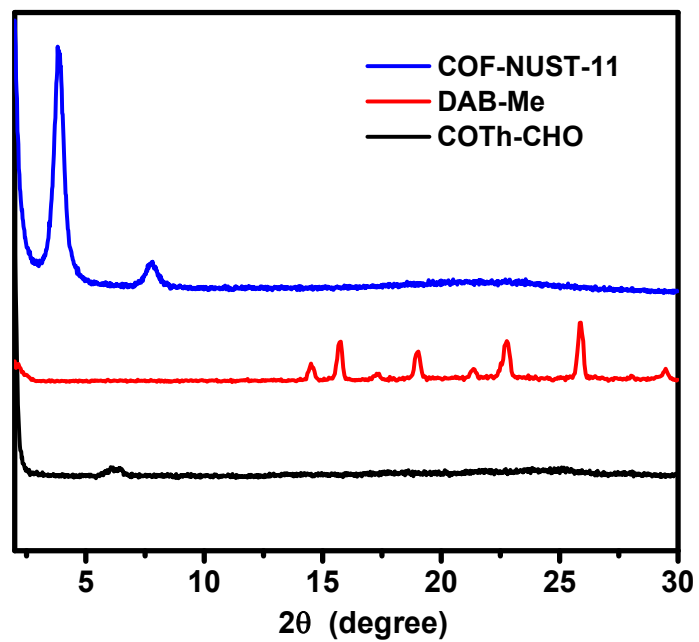


**Fig. S18** PXRD patterns of COF-NUST-11, DAB-Me, and COTh-CHO

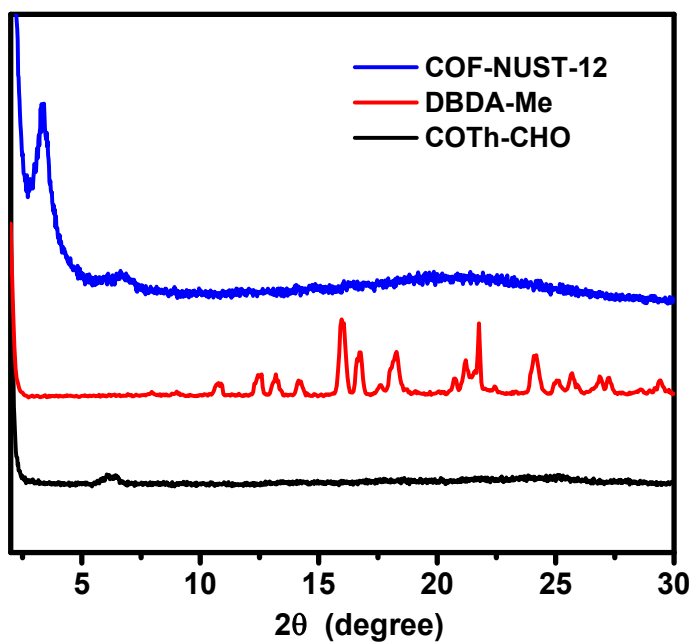


**Fig. S19** PXRD patterns of COF-NUST-12, DBDA-Me, and COTh-CHO

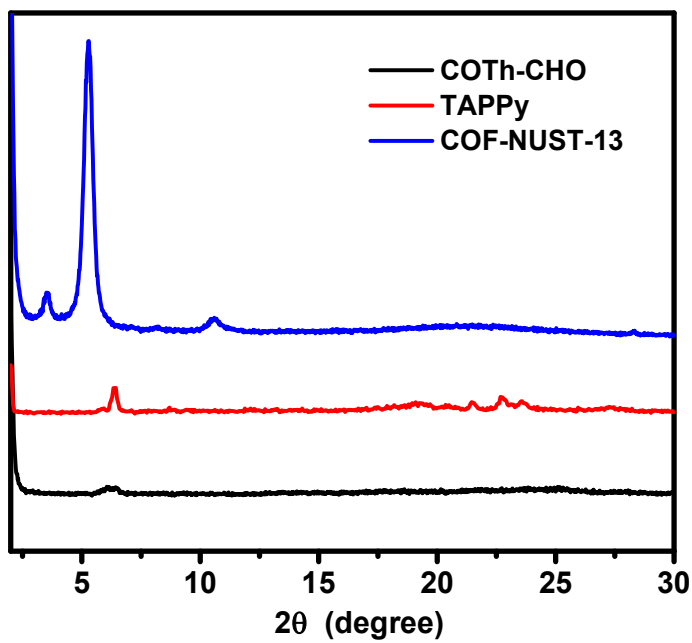


**Fig. S20** PXRD patterns of COF-NUST-13, TAPPY, and COTh-CHO

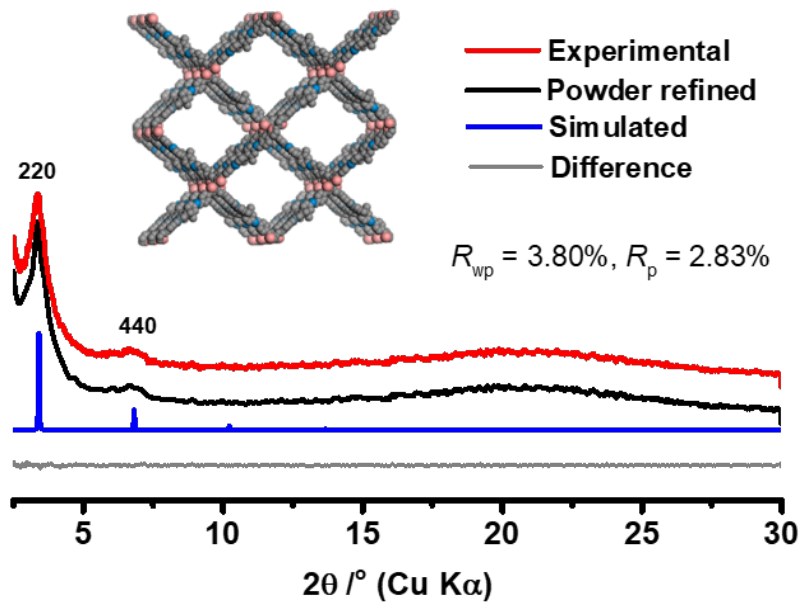


**Fig. S21** PXRD patterns of COF-NUST-12. PXRD profiles of experimental pattern (red curves), Pawley refined (black curves), calculated (green curves) patterns, and their difference (gray curves)

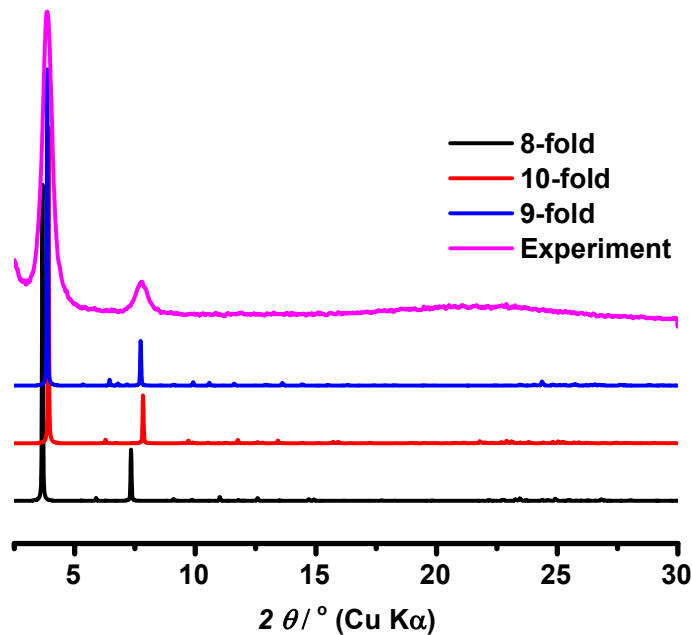


**Fig. S22** Calculated PXRD pattern of COF-NUST-11 based on the 8-, 9- and 10- fold interpenetration of *dia* net

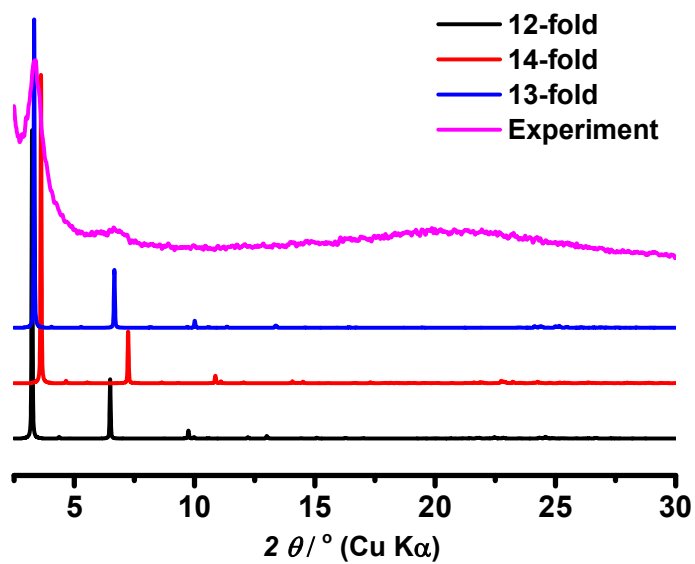


**Fig. S23** Calculated PXRD pattern of COF-NUST-12 based on the 12-, 13- and 14- fold interpenetration of *dia* net

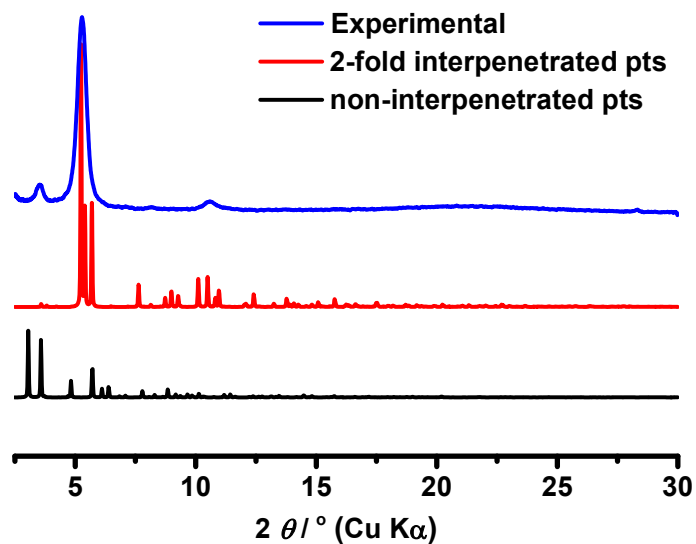


**Fig. S24** Calculated PXRD pattern of COF-NUST-13 based on the non- and 2- fold interpenetration of *pts* net

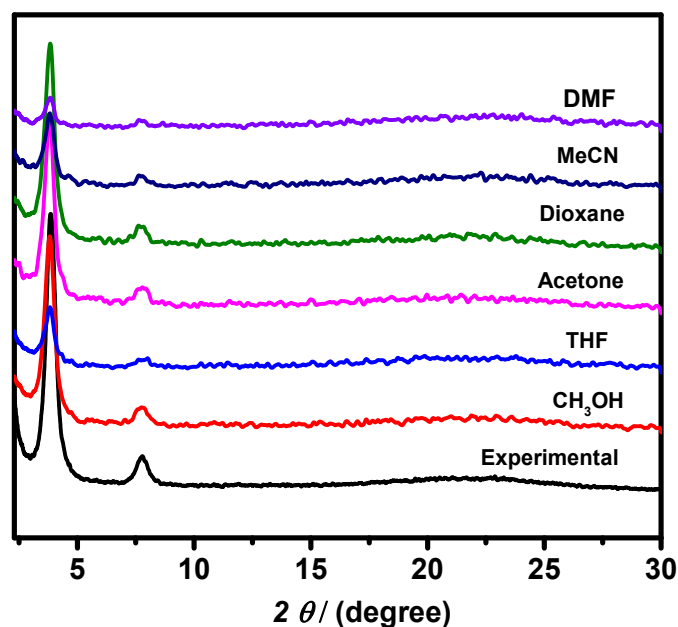


**Fig. S25** PXRD patterns of COF-NUST-11 after soaked in different solvents for 72 h

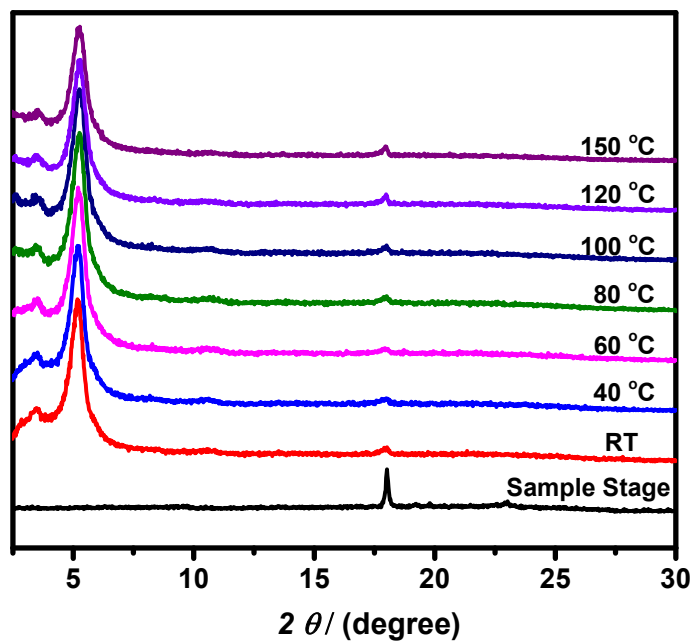


**Fig. S26** PXRD patterns of COF-NUST-13 at different temperatures

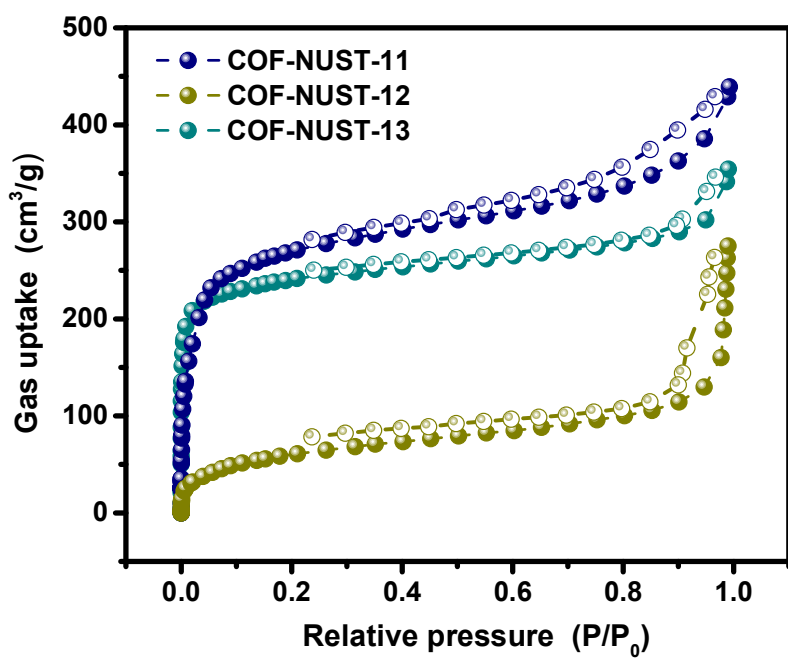


**Fig. S27** N<sub>2</sub> adsorption-desorption isotherms at 77 K of COFs

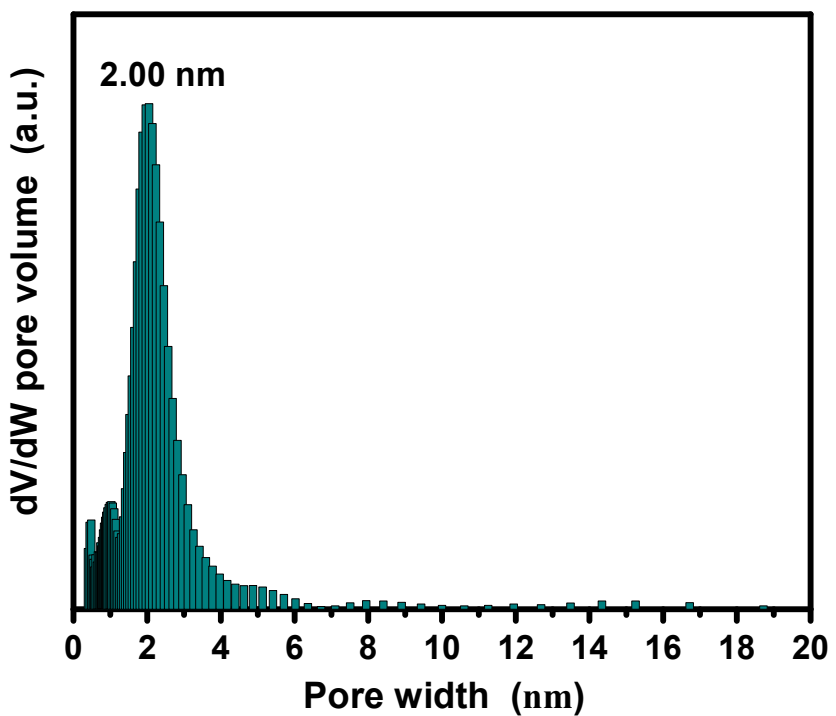


**Fig. S28** Pore size distribution of COF-NUST-11

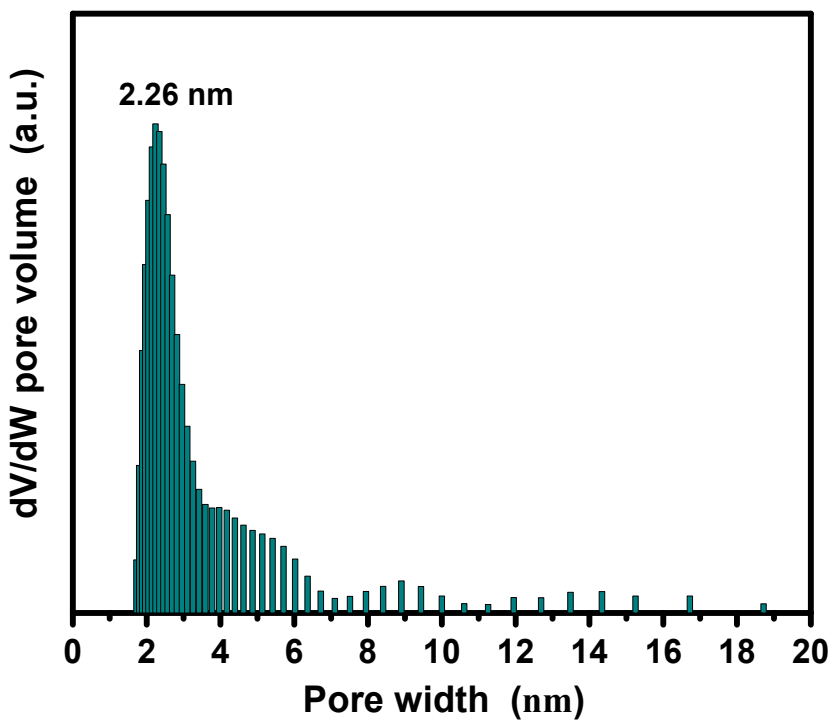


**Fig. S29** Pore size distribution of COF-NUST-12

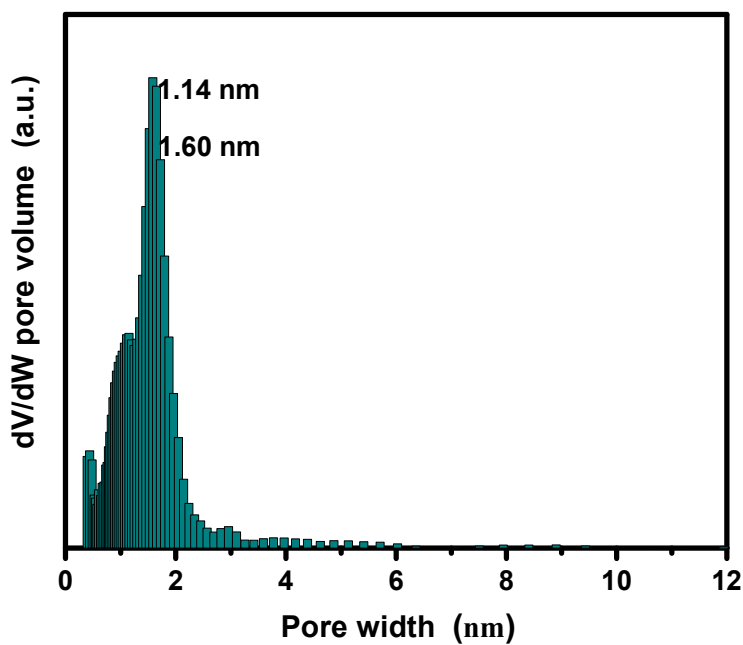


**Fig. S30** Pore size distribution of COF-NUST-13

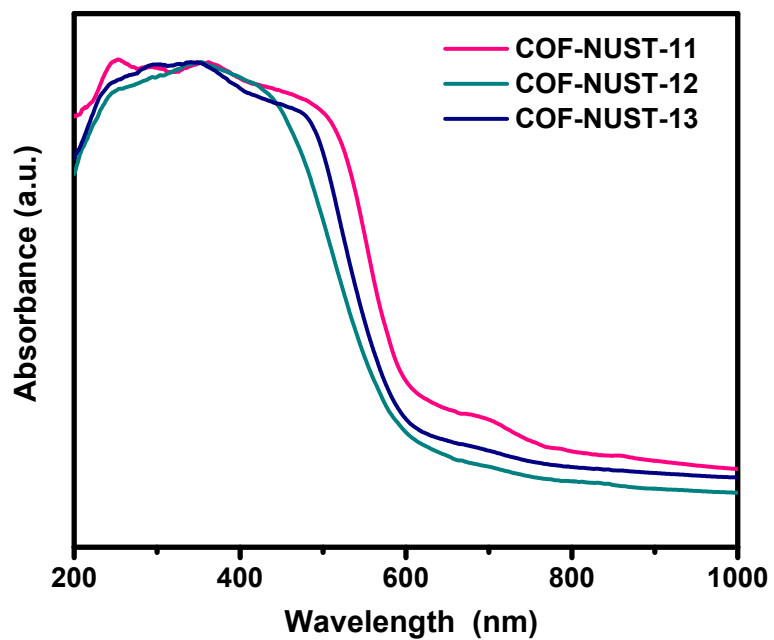


**Fig. S31** UV/vis spectra of COFs powders

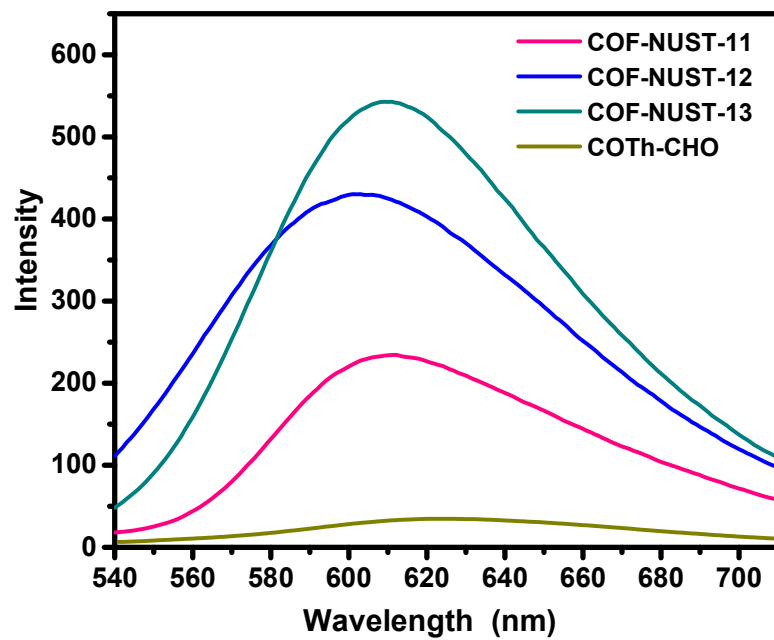


**Fig. S32** Fluorescence emission spectra of COTh-CHO, COF-NUST-11/12/13 powders ( $\lambda_{\text{ex}} = 360$  nm)

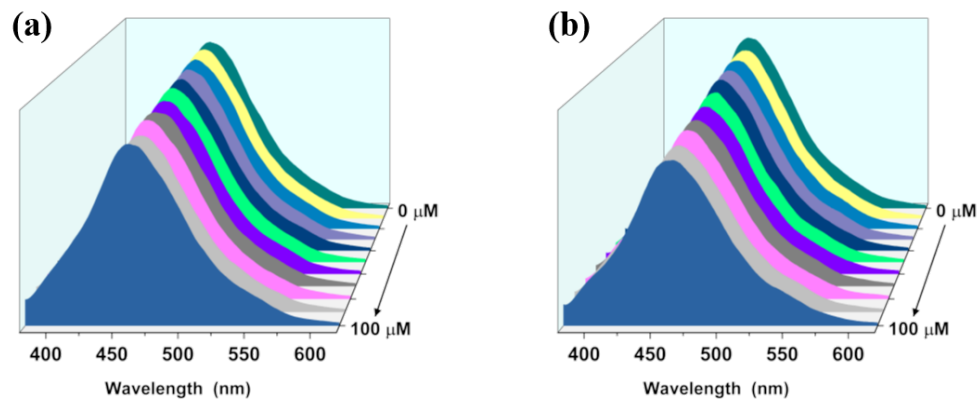


**Fig. S33** Fluorescence emission spectra of acetonitrile suspension of COF-NUST-11 upon increasing addition of (a) DNB and (b) NP ( $\lambda_{\text{ex}} = 360 \text{ nm}$ )

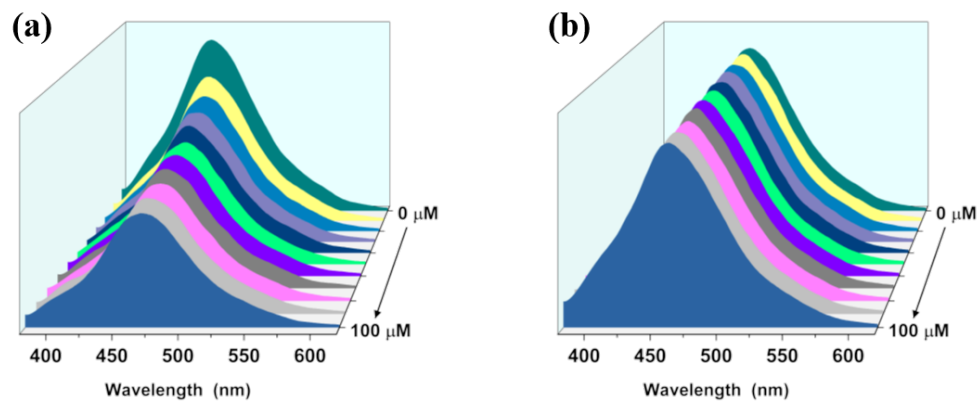


**Fig. S34** Fluorescence emission spectra of acetonitrile suspension of COF-NUST-11 upon increasing addition of (a) DNP and (b) NB ( $\lambda_{\text{ex}} = 360 \text{ nm}$ )

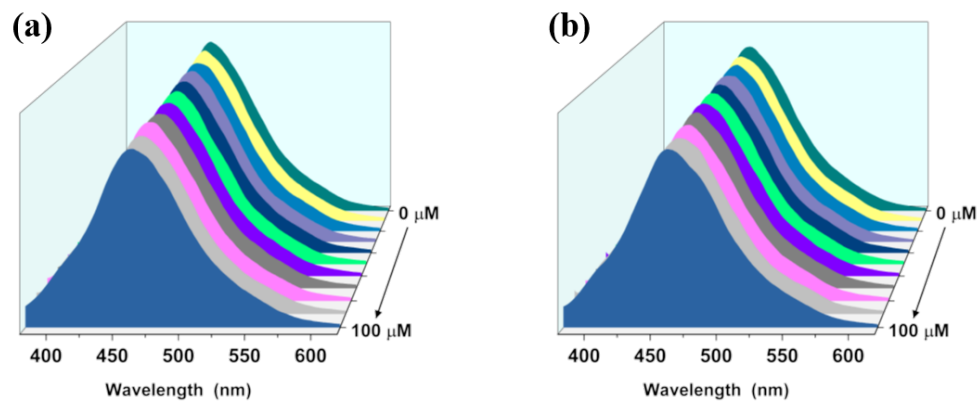


**Fig. S35** Fluorescence emission spectra of acetonitrile suspension of COF-NUST-11 upon increasing addition of (a) NT and (b) DNT ( $\lambda_{\text{ex}} = 360 \text{ nm}$ )

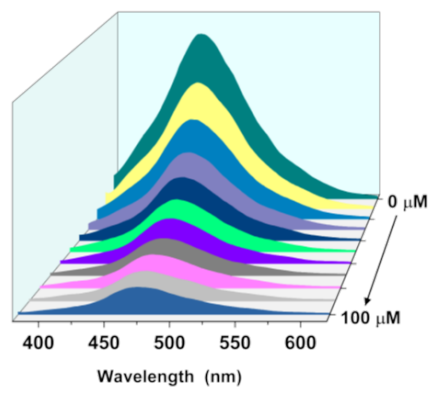


**Fig. S36** Fluorescence emission spectra of acetonitrile suspension of COF-NUST-11 upon increasing addition of TNP ( $\lambda_{\text{ex}} = 360 \text{ nm}$ )

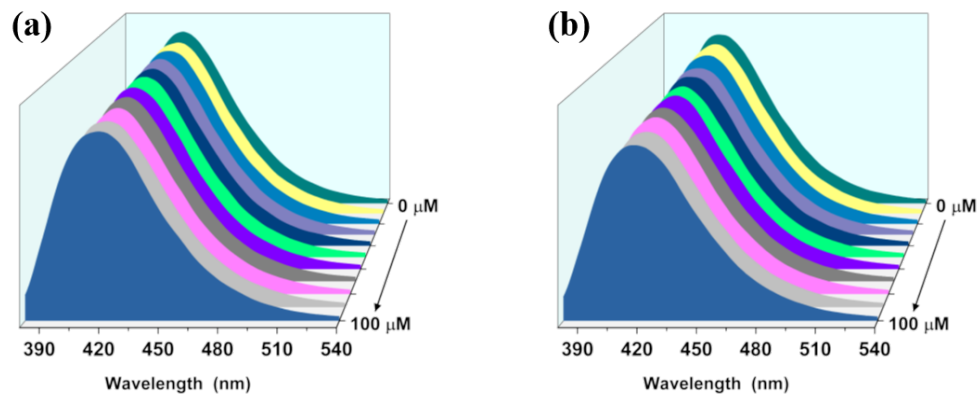


**Fig. S37** Fluorescence emission spectra of acetonitrile suspension of COF-NUST-12 upon increasing addition of (a) DNB and (b) NP ( $\lambda_{\text{ex}} = 360 \text{ nm}$ )

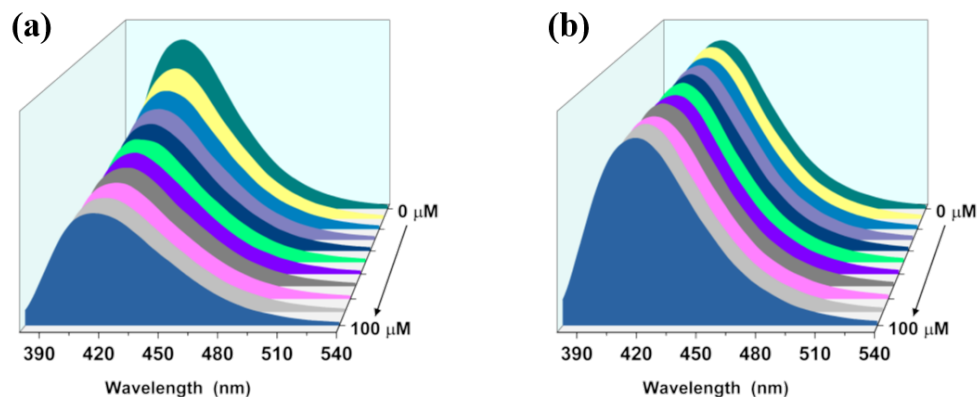


**Fig. S38** Fluorescence emission spectra of acetonitrile suspension of COF-NUST-12 upon increasing addition of (a) DNP and (b) NB ( $\lambda_{\text{ex}} = 360 \text{ nm}$ )

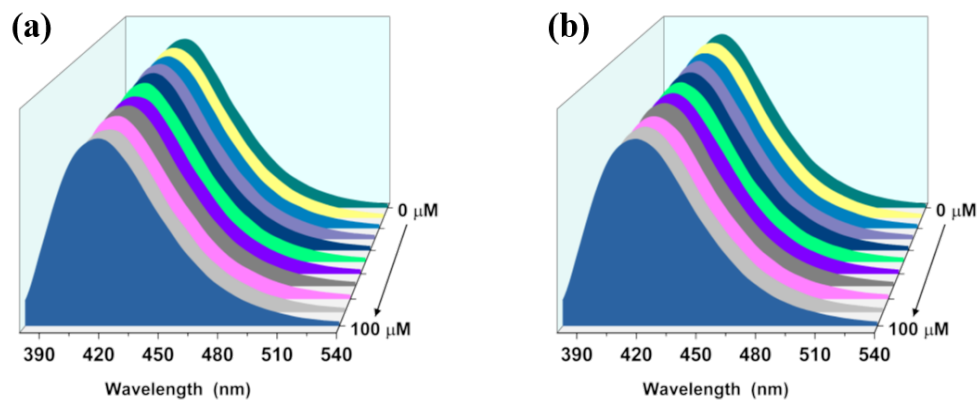


**Fig. S39** Fluorescence emission spectra of acetonitrile suspension of COF-NUST-12 upon increasing addition of (a) NT and (b) DNT ( $\lambda_{\text{ex}} = 360 \text{ nm}$ )

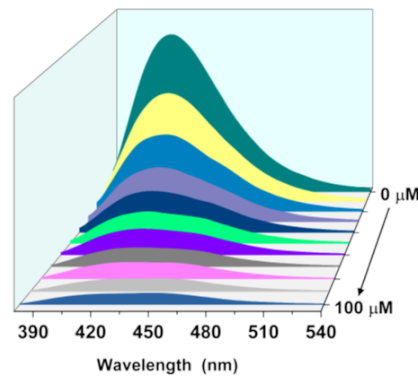


**Fig. S40** Fluorescence emission spectra of acetonitrile suspension of COF-NUST-12 upon increasing addition of TNP ( $\lambda_{\text{ex}} = 360 \text{ nm}$ )

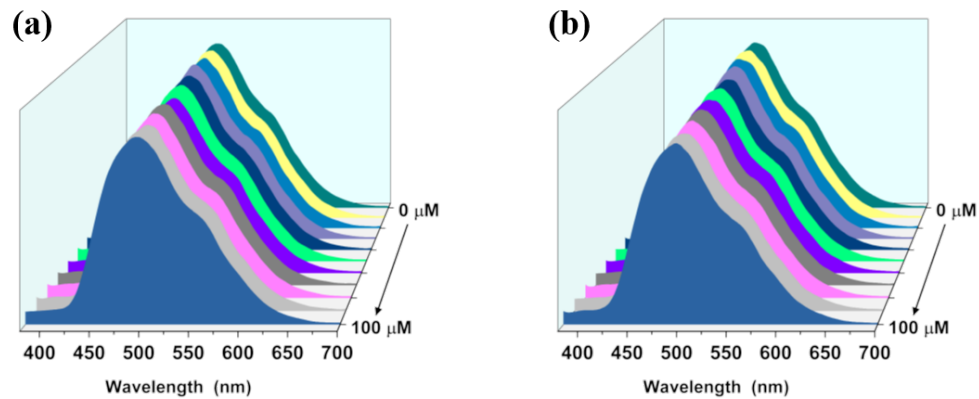


**Fig. S41** Fluorescence emission spectra of acetonitrile suspension of COF-NUST-13 upon increasing addition of (a) DNB and (b) NP ( $\lambda_{\text{ex}} = 360 \text{ nm}$ )

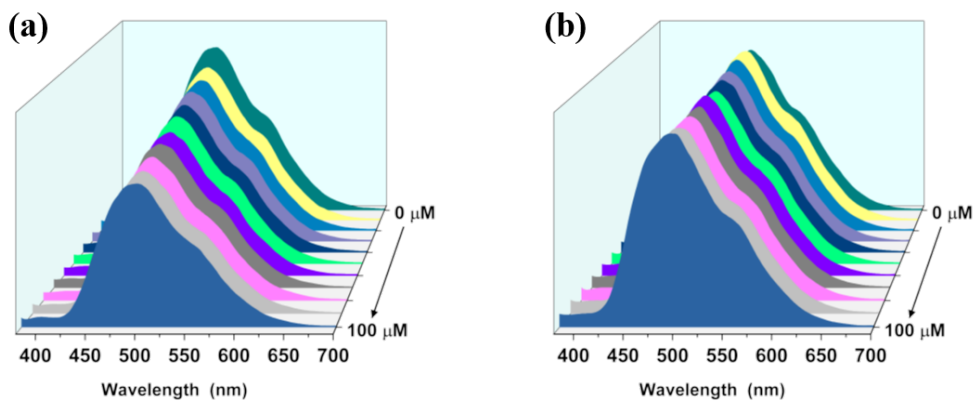


**Fig. S42** Fluorescence emission spectra of acetonitrile suspension of COF-NUST-13 upon increasing addition of (a) DNP and (b) NB ( $\lambda_{\text{ex}} = 360 \text{ nm}$ )

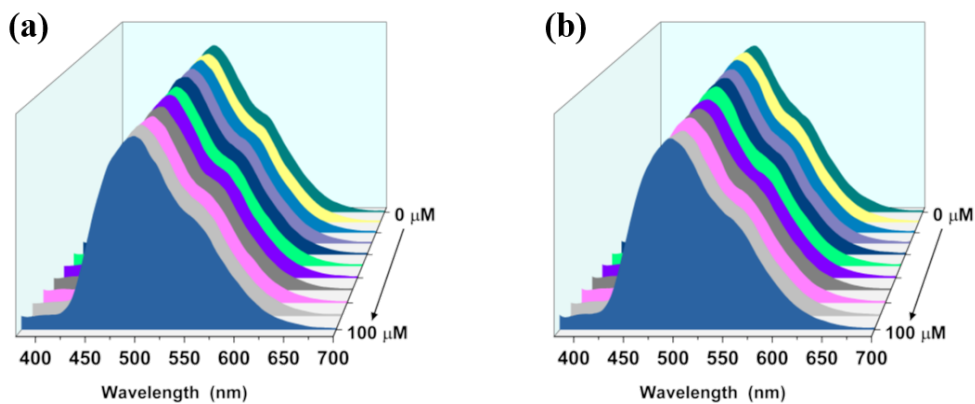


**Fig. S43** Fluorescence emission spectra of acetonitrile suspension of COF-NUST-13 upon increasing addition of (a) NT and (b) DNT ( $\lambda_{\text{ex}} = 360 \text{ nm}$ )

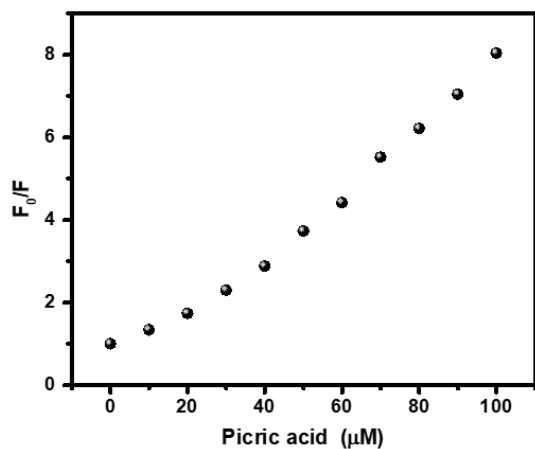


**Fig. S44** The Stern-Volmer plots obtained from titration of COF-NUST-11 with picric acid

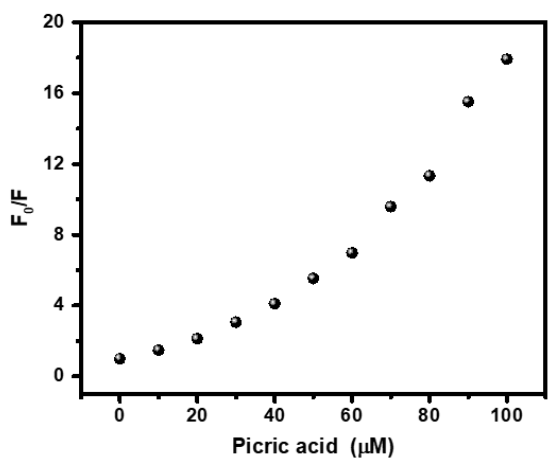


**Fig. S45** The Stern-Volmer plots obtained from titration of COF-NUST-12 with picric acid

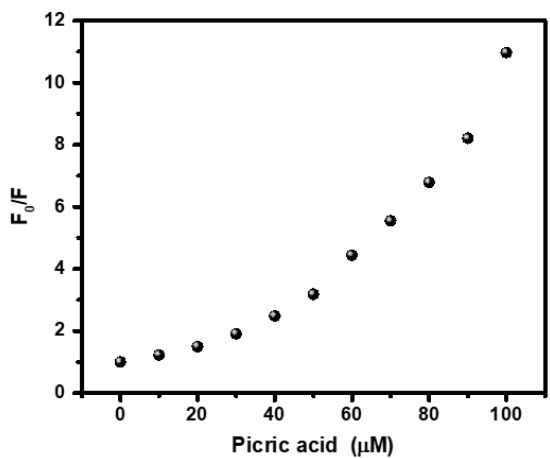


**Fig. S46** The Stern-Volmer plots obtained from titration of COF-NUST-13 with picric acid

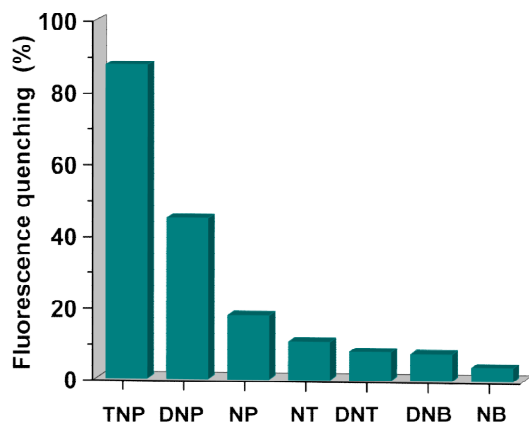


**Fig. S47** Fluorescence quenching (%) of acetonitrile suspension of COF-NUST-11 with various nitroaromatics at a concentration of 100  $\mu\text{M}$ .

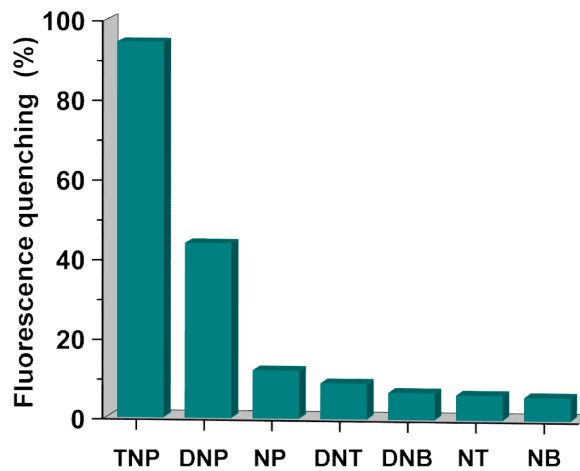


**Fig. S48** Fluorescence quenching (%) of acetonitrile suspension of COF-NUST-12 with various nitroaromatics at a concentration of 100  $\mu\text{M}$ .

**Table S3.** Fractional atomic coordinates for simulated COF-NUST-11 powders

Space group: <i>FDD2</i>			
3D orthorhombic; $a = 54.81 \text{ \AA}$ , $b = 82.79 \text{ \AA}$ , $c = 3.99 \text{ \AA}$ ; $\alpha = \beta = \gamma = 90^\circ$			
Atom	x	y	z
C1	0.43382	0.04253	4.01091
C2	0.41206	0.03903	3.83872
C3	0.39741	0.05151	3.7137
C4	0.40416	0.0677	3.76104
C5	0.42563	0.07121	3.93812
C6	0.4402	0.05882	4.06239
C7	0.38895	0.08081	3.62369
N8	0.3952	0.09576	3.67066
C9	0.3821	0.10962	3.55259
C10	0.39567	0.12199	3.40397
C11	0.38447	0.13622	3.29323
C12	0.35915	0.13819	3.33203
C13	0.34562	0.12608	3.49621
C14	0.35682	0.11182	3.60818

N15	0.34794	0.15265	3.20384
C16	0.34159	0.09953	3.79186
C17	0.39965	0.14942	3.1391
C18	0.32479	0.15486	3.15227
C19	0.31569	0.17009	3.00841
C20	0.29053	0.1722	2.97123
C21	0.28126	0.18622	2.82629
C22	0.29697	0.19853	2.71205
C23	0.32227	0.19646	2.75478
C24	0.33155	0.18238	2.90116
C25	0.2871	0.71338	7.04991
S26	0.1961	0.76978	6.97391
C27	0.2213	0.76035	6.80221
C28	0.24172	0.77033	6.79302
C29	0.23626	0.78523	6.9311
C30	0.30038	0.77937	6.39104
S31	0.3107	0.76067	6.49192
C32	0.28198	0.75548	6.63615
C33	0.26533	0.76814	6.6142
C34	0.27628	0.78142	6.46917
H35	0.40652	0.02666	3.79583
H36	0.38092	0.04853	3.5775
H37	0.43118	0.08358	3.98307
H38	0.45615	0.06219	4.20555
H39	0.37306	0.07784	3.47467
H40	0.41519	0.12043	3.37434
H41	0.32638	0.1277	3.54427
H42	0.35195	0.09422	4.00364
H43	0.33594	0.08981	3.61689

H44	0.32485	0.1051	3.89806
H45	0.39246	0.15251	2.88769
H46	0.41906	0.14578	3.11206
H47	0.39882	0.16039	3.29878
H48	0.31175	0.14535	3.20062
H49	0.27795	0.16294	3.05458
H50	0.2617	0.18724	2.8076
H51	0.33503	0.20558	2.67084
H52	0.35112	0.18105	2.92645
H53	0.24898	0.79516	6.93239
H54	0.26705	0.79277	6.43655

**Table S4.** Fractional atomic coordinates for simulated COF-NUST-12 powders

Space group: <i>FDD2</i>			
3D orthorhombic; $a = 87.11 \text{ \AA}$ , $b = 4.17 \text{ \AA}$ , $c = 66.81 \text{ \AA}$ ; $\alpha = \beta = \gamma = 90^\circ$			
Atom	x	y	z
C1	0.53001	6.85773	0.02186
C2	0.54269	7.03432	0.03147
C3	0.54172	7.12657	0.05161
C4	0.55375	7.29466	0.06062
C5	0.56691	7.37191	0.04956
C6	0.56793	7.28047	0.0295
C7	0.55588	7.11369	0.02048
C8	0.57988	7.54091	0.05866
N9	0.57923	7.65164	0.07676
C10	0.59195	7.80855	0.08615
C11	0.59012	7.93732	0.10524
C12	0.60254	8.07904	0.11501

C13	0.61716	8.09342	0.10615
C14	0.61883	7.96876	0.08646
C15	0.60633	7.82689	0.07683
C16	0.63015	8.24259	0.11759
C17	0.64174	8.40401	0.10704
C18	0.65391	8.55296	0.11685
C19	0.65478	8.547	0.13765
C20	0.64343	8.38584	0.14856
C21	0.63122	8.23351	0.13883
N22	0.66722	8.70914	0.14727
C23	0.66802	8.75268	0.16645
C24	0.68103	8.92216	0.17544
C25	0.62011	8.05625	0.1517
C26	0.63367	7.9692	0.07531
C27	0.68073	8.99443	0.19586
C28	0.69295	9.15962	0.20464
C29	0.70564	9.25355	0.1931
C30	0.70591	9.17899	0.17265
C31	0.69367	9.01533	0.16385
C32	0.71863	9.42482	0.20236
S33	0.7353	9.50544	0.19006
C34	0.74243	9.6739	0.2116
C35	0.78168	9.96077	0.22161
C36	0.76799	9.82064	0.2272
S37	0.76425	9.52503	0.28427
C38	0.75688	9.67473	0.2621
C39	0.7671	9.63596	0.24609
C40	0.7802	9.47817	0.25211
H41	0.53107	7.06452	0.06073

H42	0.55287	7.36917	0.077
H43	0.57862	7.34203	0.02043
H44	0.55682	7.0419	0.00407
H45	0.59091	7.57806	0.04979
H46	0.57844	7.92713	0.11292
H47	0.60096	8.18665	0.13056
H48	0.60796	7.72506	0.06114
H49	0.64134	8.41563	0.09
H50	0.6632	8.68026	0.10784
H51	0.64405	8.37763	0.1656
H52	0.6585	8.65857	0.17658
H53	0.62481	7.80719	0.15508
H54	0.60866	8.0336	0.14355
H55	0.61835	8.19247	0.16631
H56	0.63162	8.05346	0.0593
H57	0.63863	7.71649	0.0751
H58	0.64209	8.13799	0.08301
H59	0.6705	8.91862	0.20539
H60	0.69266	9.21895	0.22129
H61	0.71617	9.25205	0.16309
H62	0.69399	8.95751	0.14718
H63	0.79165	9.97132	0.23264
H64	0.78983	9.43146	0.24094

**Table S5.** Fractional atomic coordinates for simulated COF-NUST-13 powders

Space group: <i>P2/M</i>			
3D monoclinic; $a = 22.63 \text{ \AA}$ , $b = 49.06 \text{ \AA}$ , $c = 23.00 \text{ \AA}$ ; $\alpha = \gamma = 90^\circ$ , $\beta = 88.55^\circ$			
Atom	x	y	z

C1	0.10667	0.29492	0.10522
C2	0.12007	0.28056	0.0513
C3	0.07376	0.26342	0.0303
C4	0.02389	0.2643	0.0699
S5	0.03552	0.28575	0.12944
C6	0.14486	0.31603	0.14137
C7	0.20662	0.32209	0.13224
C8	0.23813	0.34142	0.1682
C9	0.21003	0.35633	0.21554
C10	0.14882	0.35015	0.22374
C11	0.11804	0.33094	0.18893
C12	0.23762	0.37897	0.25626
C13	0.38009	0.44897	0.37715
C14	0.41187	0.42811	0.34677
C15	0.38351	0.40783	0.31158
C16	0.32125	0.40654	0.30388
C17	0.28918	0.42711	0.33476
C18	0.31756	0.4475	0.36948
N19	0.29445	0.38535	0.26466
C20	0.41004	0.47438	0.40761
C21	0.45526	0.47487	0.45322
C22	0.47849	0.45114	0.47775
C23	0.1147	0.78611	0.9003
S24	0.04869	0.77544	0.87179
C25	0.03132	0.75379	0.93092
C26	0.07611	0.75373	0.97294
C27	0.12244	0.77209	0.95473
C28	0.1561	0.80801	0.868
C29	0.14746	0.81711	0.80887

C30	0.18375	0.83744	0.77914
C31	0.23118	0.85055	0.80662
C32	0.2396	0.84144	0.86557
C33	0.20402	0.82097	0.89488
C34	0.27128	0.874	0.77916
C35	0.38174	0.94866	0.63117
C36	0.35163	0.92807	0.60093
C37	0.31869	0.90691	0.63124
C38	0.31345	0.90443	0.69395
C39	0.34393	0.92478	0.72452
C40	0.37629	0.94614	0.69421
N41	0.27624	0.8824	0.7228
C42	0.41085	0.9744	0.59956
C43	0.45484	0.97492	0.54958
C44	0.47852	0.95116	0.52389
H45	0.16193	0.28284	0.02721
H46	0.23116	0.31173	0.0972
H47	0.28465	0.3449	0.15834
H48	0.12353	0.36045	0.25841
H49	0.07151	0.32788	0.1996
H50	0.2047	0.39013	0.28198
H51	0.45957	0.42798	0.34819
H52	0.41095	0.39297	0.28906
H53	0.2418	0.42797	0.33131
H54	0.28977	0.46277	0.39021
H55	0.46294	0.43194	0.46239
H56	0.16062	0.77527	0.98094
H57	0.11176	0.80836	0.78502
H58	0.17393	0.84321	0.73454

H59	0.27462	0.85042	0.88999
H60	0.21383	0.81561	0.93969
H61	0.29888	0.88381	0.81048
H62	0.35157	0.9288	0.55319
H63	0.29607	0.89228	0.60513
H64	0.34181	0.92469	0.77224
H65	0.39705	0.9612	0.72082
H66	0.46382	0.93195	0.54119
C67	0.39007	0.5	0.38794
C68	0.47759	0.5	0.47648
C69	0.39186	0	0.6221
C70	0.47729	0	0.52486
H71	1.35807	1.5	1.3537
H72	1.64117	1	2.34196

## Reference

- 1 H. Wang, Y. Cheng, Y. Wang, Z. Wang, D. Zhao and Z. Wang, *Synlett*, 2007, **2007**, 2390-2394.
- 2 A. Meyer, E. Sigmund, F. Luppertz, G. Schnakenburg, I. Gadaczek, T. Bredow, S. S. Jester and S. Hoger, *Beilstein J Org Chem*, 2010, **6**, 1180-1187.
- 3 Y. Wang, D. Gao, J. Shi, Y. Kan, J. Song, C. Li and H. Wang, *Tetrahedron*, 2014, **70**, 631-636.